

MICROCOPY RESOLUTION TEST CHART  
NATIONAL BUREAU OF STANDARDS-1963-A

A2445-050  
Interim Technical Report

**LEVEL**

12

AC83493 SC

PASSIVE TARGET DETECTION  
MEASUREMENTS AT 220 GHz .

AD A 093682

NEAR MILLIMETER WAVE  
RADAR TECHNOLOGY

M. L. Foster, R. E. Forsythe,  
J. M. Welch, J. M. Schuchardt

SECRET  
JAN 12 1981  
C

CONTRACT NO. DAAK70-79-C-0108

AUGUST 1980

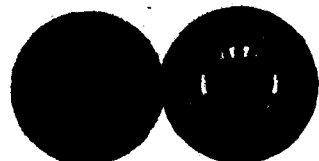
**GEORGIA INSTITUTE OF TECHNOLOGY**

Engineering Experiment Station  
Atlanta, Georgia 30332

DDG FILE COPY

GT  
EES

DISTRIBUTION STATEMENT A  
Approved for public release;  
Distribution Unlimited



80 11 12 057

12

Project No. A-2445-050

6

Passive Target Detection Measurements at 220 GHz

9

Criteria technical report

10

M.L. Foster, R.E. Forsythe, J.M. Welch and J.M. Schuchardt  
Engineering Experiment Station  
Georgia Institute of Technology  
Atlanta, Georgia 30332

RECEIVED  
JAN 12 1981  
D

11

August 1980

12

64

15

Contract No. DAAK78-79-C-0108  
Army Night Vision Laboratory  
Laser Division  
Fort Belvoir, Virginia

DISTRIBUTION STATEMENT A  
Approved for public release;  
Distribution Unlimited

153850

1/3

SECURITY CLASSIFICATION OF THIS PAGE (When Data Entered)

REPORT DOCUMENTATION PAGE		READ INSTRUCTIONS BEFORE COMPLETING FORM
1. REPORT NUMBER	2. GOVT ACCESSION NO. <i>AD-A093 682</i>	3. RECIPIENT'S CATALOG NUMBER
4. TITLE (and Subtitle) Passive Target Detection Measurements at 220 GHz		5. TYPE OF REPORT & PERIOD COVERED
		6. PERFORMING ORG. REPORT NUMBER
7. AUTHOR(s) M.L. Foster, R.E. Forsythe, J.M. Welch, J.M. Schuchardt		8. CONTRACT OR GRANT NUMBER(s) DAAK70-79-C-0108'
9. PERFORMING ORGANIZATION NAME AND ADDRESS Georgia Institute of Technology Engineering Experiment Station/ Atlanta, Georgia 30332		10. PROGRAM ELEMENT, PROJECT, TASK AREA & WORK UNIT NUMBERS
11. CONTROLLING OFFICE NAME AND ADDRESS Army Night Vision Laboratory Laser Division Fort Belvoir, Virginia		12. REPORT DATE August, 1980
		13. NUMBER OF PAGES
14. MONITORING AGENCY NAME & ADDRESS (if different from Controlling Office)		15. SECURITY CLASS. (of this report)
		15a. DECLASSIFICATION DOWNGRADING SCHEDULE
16. DISTRIBUTION STATEMENT (of this Report)		
17. DISTRIBUTION STATEMENT (of the abstract entered in Block 20, if different from Report)		
18. SUPPLEMENTARY NOTES		
19. KEY WORDS (Continue on reverse side if necessary and identify by block number) Radiometer, 220 GHz, Target Detection, Sky temperature.		
20. ABSTRACT (Continue on reverse side if necessary and identify by block number) Passive target signature measurements were performed at 220 GHz and 95 GHz. Test results show target detection is possible even with very warm sky temperatures.  A 220 GHz/94 GHz sensor was used to detect a metallic vehicle at a range of 300 meters during the summer, of 1980 at an Army facility (Fort Gillem) near Atlanta. Using a raster scan format, scans were made above, through and below the target. The scene thus viewed included trees and grass. Measurements were also made of the overhead sky and calibrated hot and cold radiometer loads.		

SECURITY CLASSIFICATION OF THIS PAGE(When Data Entered)

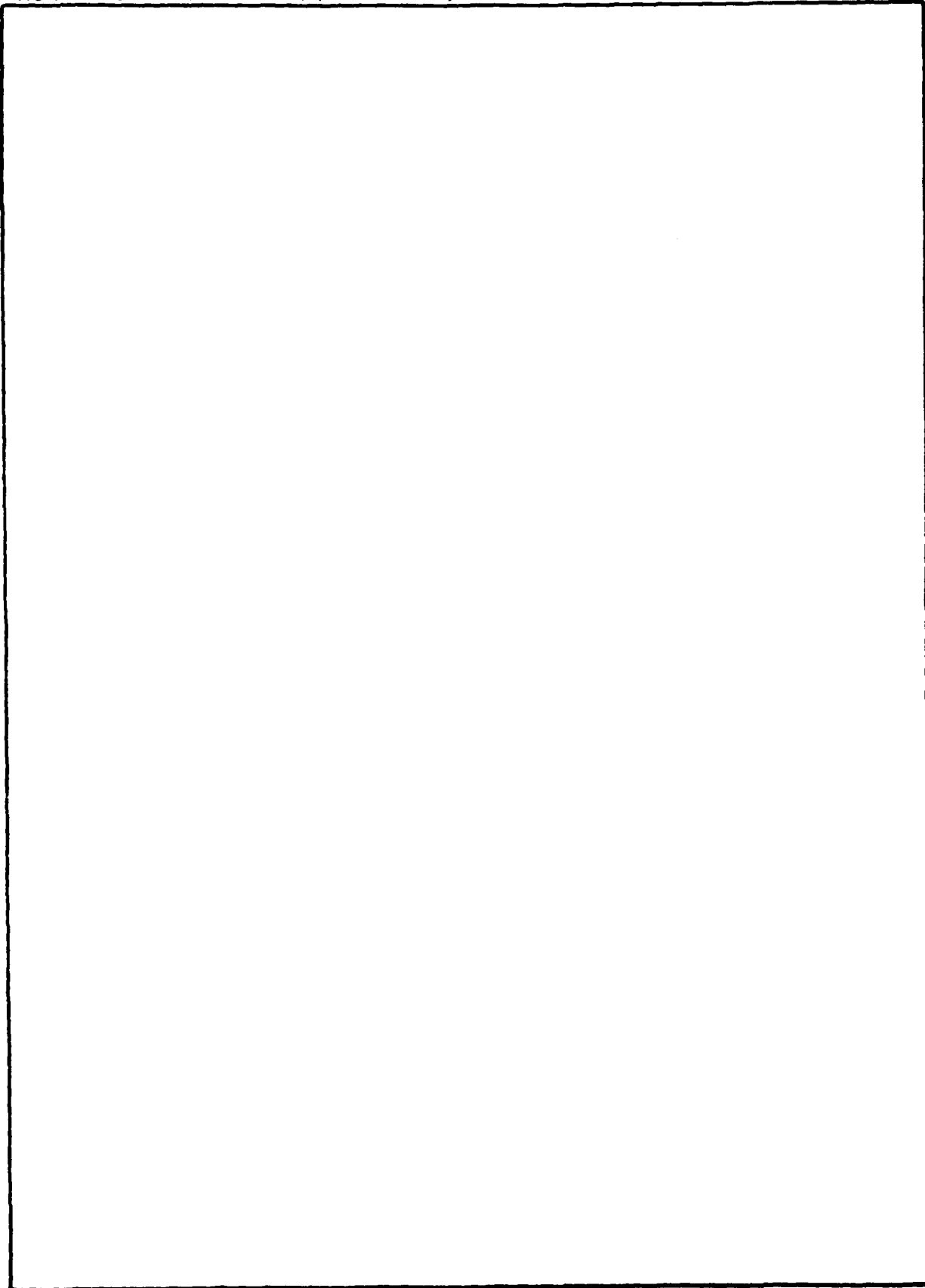


## Table of Contents

Section	Title	Page
1.0	Introduction	1
2.0	Target Detectability Considerations	5
2.1	System Performance	5
2.2	Sky Temperatures	5
2.3	Expected Temperature Differentials for Target Detection	10
3.0	Test Site and Target	14
3.1	Test Site	14
3.2	Target	14
3.3	Radiometer Sensor	14
3.4	Scan Raster	14
3.5	Measurements Schedule	17
4.0	Data	18
4.1	Data Format	18
4.2	Target Detection	18
5.0	Acknowledgment	23
Appendix A1	Detailed Radiometer Description	24
Appendix A2	Measurements Log	40
Appendix A3	Target Scans	42
Appendix A4	Data Tape Format	50

Accession For	
NSIC CRARI	<input checked="" type="checkbox"/>
ERIC TIB	<input type="checkbox"/>
Unannounced	<input type="checkbox"/>
Justification	<input type="checkbox"/>
By _____	
Distribution/	
Availability Codes	
Dist	Special
A	

## List of Illustrations

Figure	Title	Page
1	Target Contrast and Background Factors	2
2	Effect of Lens Loss on Radiometer Output	9
3	Target Reflecting Geometry	11
4	Test Site Geometry	15
5	Test Site Photograph	16
6	Raster Scan Geometry	19
7	Target Detection Strip Chart	20
8	94 GHz Digital Image	21
9	220 GHz Digital Image	22

## List of Tables

Table	Title	Page
1	Target Contrast and Required Radiometer Sensitivity	3
2	System $\Delta T_{\min}$	6
3	Sky Temperature at Test Site	7
4	Expected Target Contrasts	13

## 1.0 Introduction

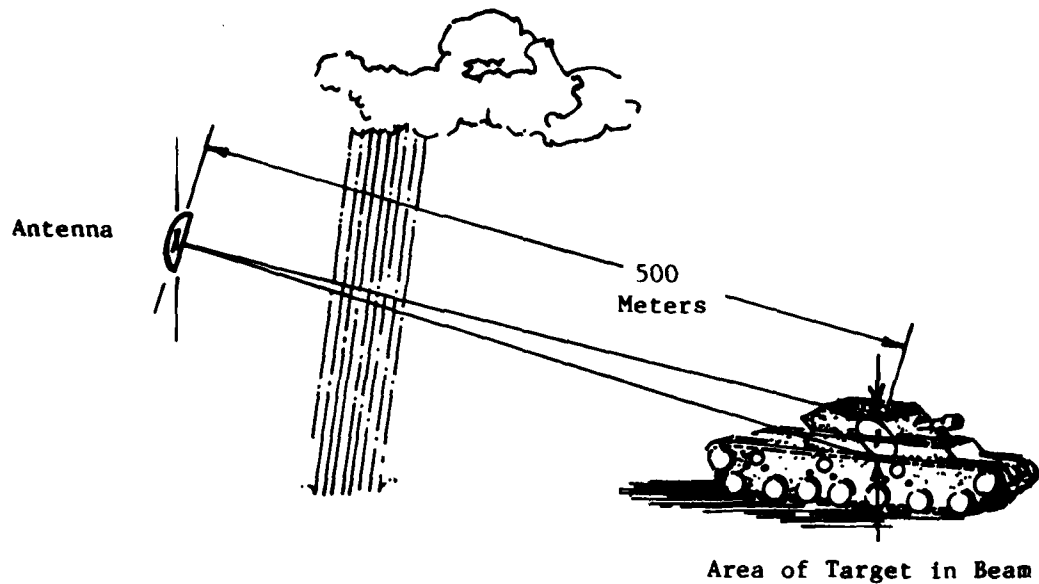
There is a need for passive high resolution millimeter wave sensor data at 220 GHz so that the Army can utilize 220 GHz sensors for tactical applications. Such sensors could stand alone or be used in conjunction with active sensors. The use of a combination of sensors offers the possibility for good all-weather operation and reduced visibility in the passive mode.

Calculations indicate that adequate target detection can occur at a range of 500 meters using an instrument having a sensitivity such that  $\Delta T_{\min}$  is 0.5 K or better. These calculations are based on the geometry shown in Figure 1. For the typical situations listed in Table 1 we see that target detectability is very good in clear weather and degrades as the weather deteriorates. For the warm sky condition shown, adequate target contrasts exists for low error detection.

This report covers results of field measurements over a medium range (250 m) using an imaging 220 GHz radiometer. These were preliminary tests designed to assess the detectability of a target at ranges in excess of 250 m. The tests utilized the Georgia Tech instrumentation radiometer modified by the installation of a 220 GHz front end. The tests were conducted at an Army facility in Atlanta in the early summer of 1980.

The weather at the site during the tests was extremely hot and humid. The measured data also indicate the radiometric sky temperature was quite warm, a situation not totally expected in summer conditions. This condition was similar to that calculated for an intense fog and represented an extreme condition. To provide additional target data under these conditions simultaneous measurements were made at 95 GHz. Test results indicate good target detections at both 220 GHz and 95 GHz.

Section 2.0 discusses some of the important considerations in evaluating target detectability. Section 3.0 describes the test conditions and test site. Section 4.0 presents the data obtained.



a) Target/Environment Geometry

$$\text{Target Contrast} = T_{TGT} - T_B(\text{Apparent})$$

$$T_{TGT} = \frac{r(T_S + T_B)A + ST_B}{L_{ATM}} + T_{ATM}\left(1 - \frac{1}{L_{ATM}}\right)$$

$$T_B(\text{Apparent}) = \frac{T_B}{L_{ATM}} + T_{ATM}\left(1 - \frac{1}{L_{ATM}}\right)$$

- $T_{TGT}$  = Apparent Radiometric Temperature of Target.
- $T_B$  = Radiometric Temperature of Background.
- $T_B(\text{Apparent})$  = Apparent Radiometric Temperature of Background as Modified by Atmospheric Loss  $L_{ATM}$ .
- $r$  = Averaging Constant to Account for Average Apparent Radiometric Temperature of Target Surface (Part of Target Surface Reflects the Sky and Part Reflects the Background)  $r = 1/2$  assumed.
- $T_S$  = Radiometric Sky Temperature
- $A$  = Beam Filling Factor of Target  
 $\leq \frac{\text{Area of Target in Beam}}{\text{Area of Beam Spot}}$
- $S$  = Beam Spillover =  $1 - A$
- $L_{ATM}$  = Loss of Atmosphere Between Target and Radiometer.
- $T_{ATM}$  = Physical Temperature of Atmosphere Between Target and Radiometer  $T_{ATM} = 290$  K.

b) Target Contrast Equations and Terms

Figure 1. Target Contrast and Background Factors.

TABLE 1  
 TARGET CONTRAST AND REQUIRED RADIONETER SENSITIVITY

TARGET* CONTRAST (ANTENNA DIA.)	$\Delta T_{min}$ REQUIRED (S/N $\geq$ 10)	WEATHER
58.9 K (20")	5.9 K	Clear (Atmospheric Attenuation = 3 dB/km ( $T_S = 80$ K))
42.5 K (6")	4.2 K	
8 K (20")	0.8 K	Fog/ Haze (Atmospheric Attenuation = 10 dB/km ( $T_S = 200$ K))
5.6 K (6")	0.6 K	

\* Conditions  
 Range = 500 meters  
 Background Temperature = 250 K  
 Atmospheric Temperature = 290 K

In subsequent efforts to be conducted under this program, a new more sensitive RF front-end operating at 220 GHz will be developed. This should permit additional measurements to be performed and more extensive target, scene and instrument tradeoffs to be made.

## 2.0 Target Detectability Considerations

### 2.1 System Performance

The standard measure of radiometer system performance is the minimum detectable temperature difference ( $\Delta T_{\min}$ ). This value can be determined from a calibration as

$$\Delta T_{\min} = |G| N_{\text{RMS}} \quad (1)$$

where  $G$  is the system gain in degrees per volt and  $N_{\text{RMS}}$  is the RMS Noise in volts. The  $\Delta T_{\min}$  of a system can also be expressed as

$$\Delta T_{\min} = K T_{\text{SYS}} (B_{\text{IF}} \tau_{\text{I}})^{-1/2} \quad (2)$$

where

- $K$  = radiometer constant  
=  $\pi/\sqrt{2}$  for this system
- $T_{\text{SYS}}$  = system temperature
- $B_{\text{IF}}$  = IF bandwidth  
= 2 GHz
- $\tau_{\text{I}}$  = integration time

The  $\Delta T_{\min}$  of the instrument used in the measurement is shown in Table 2. The variations reflect primarily the change in mixers used.

### 2.2 Sky Temperatures

Sky temperatures at the test site were determined during calibration and are given in Table 3. For some calibrations there are two sky temperatures given. For the first the sky was viewed through the sky port. The second was obtained by placing a reflector in front of the large lens. There is a loss associated with this lens which is given by (in dB)

$$L = 10 \log \frac{T_{\text{S}} - T_{\text{L}}}{T_{\text{M}} - T_{\text{L}}} \quad (3)$$

- $T_{\text{S}}$  = true scene temperature
- $T_{\text{M}}$  = measured scene temperature
- $T_{\text{L}}$  = lens physical temperature

Table 2  
SYSTEM  $\Delta T_{\min}$

DATE	TIME	MIXER	$\tau_I$ (sec.)	$\Delta T_{\min}$ (K)
6-19	7:00 pm	2 diode	1.6	0.6
6-19	6:00 pm	2 diode	1.6	0.7
6-19	7:30 pm	2 diode	1.6	1.2
6-20	2:00 pm	2 diode	1.6	1.8
6-20	4:30 pm	2 diode	5.0	0.4
6-20	6:30 pm	1 diode	5.0	5.4
6-20	9:00 pm	1 diode	16.0	1.1
6-24	5:00 pm	1 diode	5.0	3.2
6-24	5:15 pm	1 diode	16.0	1.4
6-25	3:00 pm	2 diode	5.0	0.8
6-26	9:00 am	2 diode	1.6	2.4
6-26	9:30 am	2 diode	5.0	0.6
6-26	10:00 am	2 diode	5.0	0.7
6-26	5:00 pm	2 diode	5.0	0.5
6-26	6:00 pm	2 diode	5.0	0.7
6-26	6:30 pm	2 diode	5.0	0.4
6-26	7:00 pm	2 diode	5.0	0.8
6-26	7:30 pm	2 diode	5.0	0.6

2 diode mixer average  $\Delta T_{\min} = 0.87$  K

1 diode mixer average  $\Delta T_{\min} = 2.78$  K

Table 3

## SKY TEMPERATURE AT TEST SITE

Date	Temp(°C)	Relative Humidity (%)	Sky Temp (K)	
			Sky Port	Large Lens
6-19	28.9	65	292.3	306.0
6-19	28.9	65	273.8	296.6
6-19	28.9	65	276.7	296.6
6-20	30.6	64	263.4	298.2
6-20	31.1	42	239.4	NA
6-20	29.4	44	204.4	265.7
6-20	32.2	42	301.7	NA
6-24	26.7	87	279.4	296.6
6-24	26.7	87	279.4	296.6
6-25	28.9	87	289.4	NA
6-26	27.8	61	264.7	NA
6-26	28.3	61	255.2	NA
6-26	31.7	53	258.1	NA
6-26	31.1	56	241.8	NA
6-26	29.4	63	270.2	NA
6-26	28.9	61	263.4	NA
6-26	32.2	50	263.2	NA
6-26	31.7	53	264.6	NA

Values for L using this formula range from 3.8 dB to 7.0 dB.\* The lens loss effect is shown in Figure 2. The radiometer is calibrated internally and thus does not include lens loss. This calibration produces a straight line as shown in Figure 2. When lens loss is introduced, the radiometer output follows a second straight line. The two lines intersect at  $T_{LENS}$ . As can be seen, the effect of lens loss is to shift the apparent temperature of the scene toward the lens temperature. Equation 3 is used to correct for this effect.

In order to assess the relationship between apparent sky temperature and the air temperature and humidity, the correlation coefficient can be calculated. The correlation coefficient between two variables X and Y is defined as

$$cc = \frac{\sum_{i=1}^n (X_i - \bar{X})(Y_i - \bar{Y})}{\left[ \left( \sum_{i=1}^n (X_i - \bar{X})^2 \right) \cdot \left( \sum_{i=1}^n (Y_i - \bar{Y})^2 \right) \right]^{1/2}}$$

where  $\bar{X}$  and  $\bar{Y}$  are the means of X and Y. The correlation coefficient can vary between 1 and -1 with 1 indicating strong positive correlation, -1 strong negative correlation and 0 no correlation.

The correlation coefficient between sky temperature and surface level humidity gives  $cc = 0.44$ . This indicates that there is probably a relation between humidity and sky temperature. However, it is either not strictly linear or there are other factors involved.

The correlation coefficient between sky temperature and air temperature is  $cc = 0.17$ . This indicates that air temperature differences of the order encountered in this test have little effect on sky temperature.

\* Based on extensive measurements made using this same sensor at 95 GHz, the expected loss is  $\frac{220}{95} \times 1.7 \text{ dB} = 3.9 \text{ dB}$ . Measured values exceeded this expected value because of normal measurement uncertainty and a small amount of local oscillator leakage that is reflected back into the receiver. The use of either a pure reflector antenna or a lens made from a lower loss material such as TPX appears in order for 220 GHz sensors.

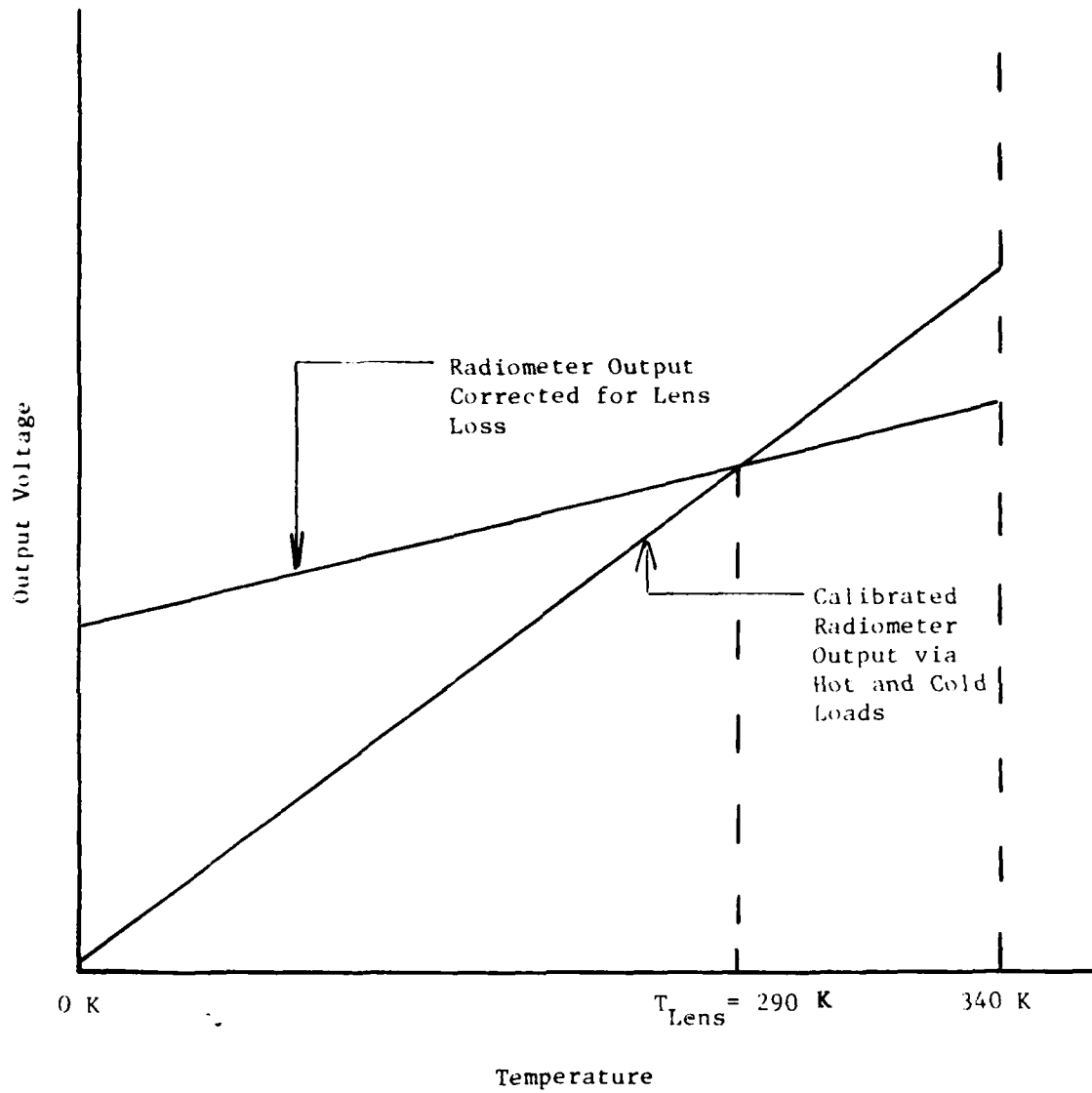


Figure 2. Effect of Lens Loss on Radiometer Output.

### 2.3 Expected Temperature Differentials for Target Detection

The difference between the target apparent temperature and the background temperature determines whether a target detection is possible. This difference,  $T_D$ , is determined at the radiometer output. The apparent target temperature has a value between the sky temperature and the background temperature. It is determined by the beamfill factor,  $A$ , and an averaging constant,  $r$ , to account for the fact that part of the target reflects the sky and part reflects the background. The target is assumed to be perfectly reflective. For the target and range used in these tests (a petroleum tanker) the beamfill is estimated to be 1. Figure 3 shows the target geometry as it relates to the averaging constant. The figure shows the condition for the maximum value of  $r$ . Specular reflection is assumed and ray tracing is used to estimate the averaging constant. For the geometry shown, the averaging constant is estimated to be 0.5. The target temperature is thus given by

$$T_T = r(T_S + T_B) = 0.5(T_S + T_B)$$

where

$T_T$  = target temperature

$T_S$  = sky temperature

$T_B$  = background temperature

This temperature is modified by two loss factors to produce the radiometer output. The first loss factor is the atmospheric path loss,  $L_{ATM}$ , between the target and the radiometer. The apparent target temperature after this loss is given by

$$T_{TI} = \frac{T_T}{L_{ATM}} + T_{ATM} \left(1 - \frac{1}{L_{ATM}}\right)$$

Referring to Table 1, the atmospheric path loss at 300 m would be 3 dB for the conditions experienced in these tests. As a ratio, path loss is  $L_{ATM} = 2$ . The lens loss,  $L_{LENS}$ , correction is then applied to this resulting apparent temperature. Lens loss correction must be made since the internal calibrations do not take the lens loss into account. However, all other RF losses are calibrated out. The apparent target temperature at the radiometer input is thus given by

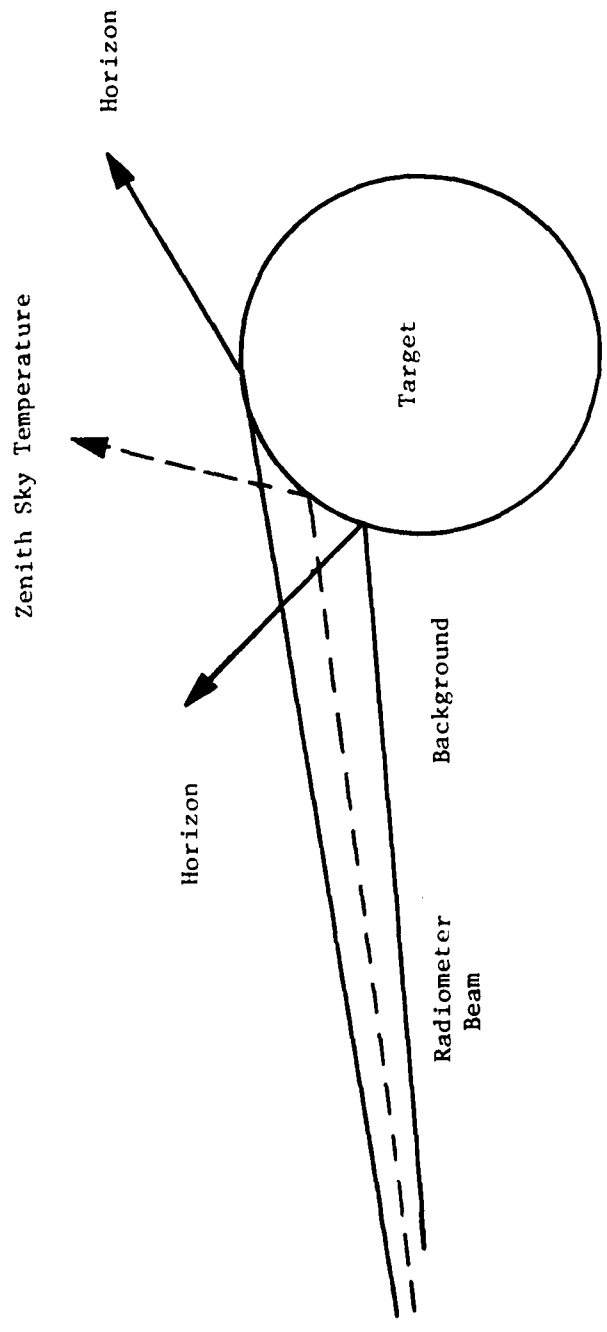


Figure 3. Target Reflecting Geometry.

$$T_{APP} = \frac{T_{TI}}{L_{LENS}} + T_{LENS} \left(1 - \frac{1}{L_{LENS}}\right)$$

Table 4 gives the expected target contrast  $\Delta T_D$  for various combinations of sky and ambient temperatures typical of the conditions during these tests. As can be seen from this table,  $\Delta T_D$  is fairly low for this range of sky temperatures and ambient temperatures. The signal to noise ratio for a target detecting radiometer is normally defined as

$$S/N(\text{db}) = 10 \log \frac{\Delta T_D}{\Delta T_{\min}}$$

Using a value of  $\Delta T_{\min} = 0.87$  K (see Table 2) and a maximum  $\Delta T_D = 8$  K (see Table 4), the signal to noise ratio for these examples is at most 9.6 dB.

Table 4  
 Expected Target Contrasts

$T_s$	$T_B$	$T_{APP}$	$\Delta T_D = T_B - T_{APP}$
260 K	300 K	292 K	8 K
270	300	294	6
280	300	296	4
260	290	284	6
270	290	286	4
280	290	288	2

$T_s$  = Sky Temperature  
 $T_B$  = Background Temperature  
 $T_{APP}$  = Apparent Target Temperature

### 3.0 Test Site and Target

#### 3.1 Test Site

The tests were conducted at the U. S. Army facility at Fort Gillem on an unused airstrip. The radiometer was set up on the airstrip in a geometry shown in Figure 4. The target was located 305 meters away in a grassy field at the end of the airstrip. Behind the target is a wooded area so that a scan of the target and its surroundings would view only the target or vegetation surrounding the target. A photograph of the target taken from the radiometer location is shown in Figure 5. The framed portion of the photograph is the area actually scanned by the radiometer.

#### 3.2 Target

The target for these tests was a gasoline tanker trailer. It was approximately 12.2 meters long and 2 meters in diameter. At 305 m it subtended an angle of  $2.3^{\circ} \times 0.4^{\circ}$ . The surface was unpainted metal.

#### 3.3 Radiometer Sensor

The Georgia Tech instrumentation radiometer is a Dicke radiometer operating simultaneously at two frequencies (95 GHz and 220 GHz in these tests). The two frequencies share a single 20-inch lens by use of a special rotating reflective chopper blade. The 95 GHz portion has four channels utilizing two bandwidths on each of two orthogonal polarizations. The 220 GHz portion has a single output channel.

The radiometer features a computer controlled internal calibration system. The radiometer views various temperature controlled loads and also a sky reflector by positioning reflective blades in the path of the beam.

The radiometer is positioned by a computer controlled elevation-over-azimuth positioner. Other features include a television camera, digital data recording and remote operation. Further information on the Georgia Tech instrumentation radiometer is given in Appendix A1.

#### 3.4 Scan Raster

The tests were done by scanning a raster of 10 lines. The raster is approximately centered on the center of the target and is  $3.8^{\circ}$  wide by  $2.0^{\circ}$  high. The scan lines are thus  $0.2^{\circ}$  apart (equivalent to the

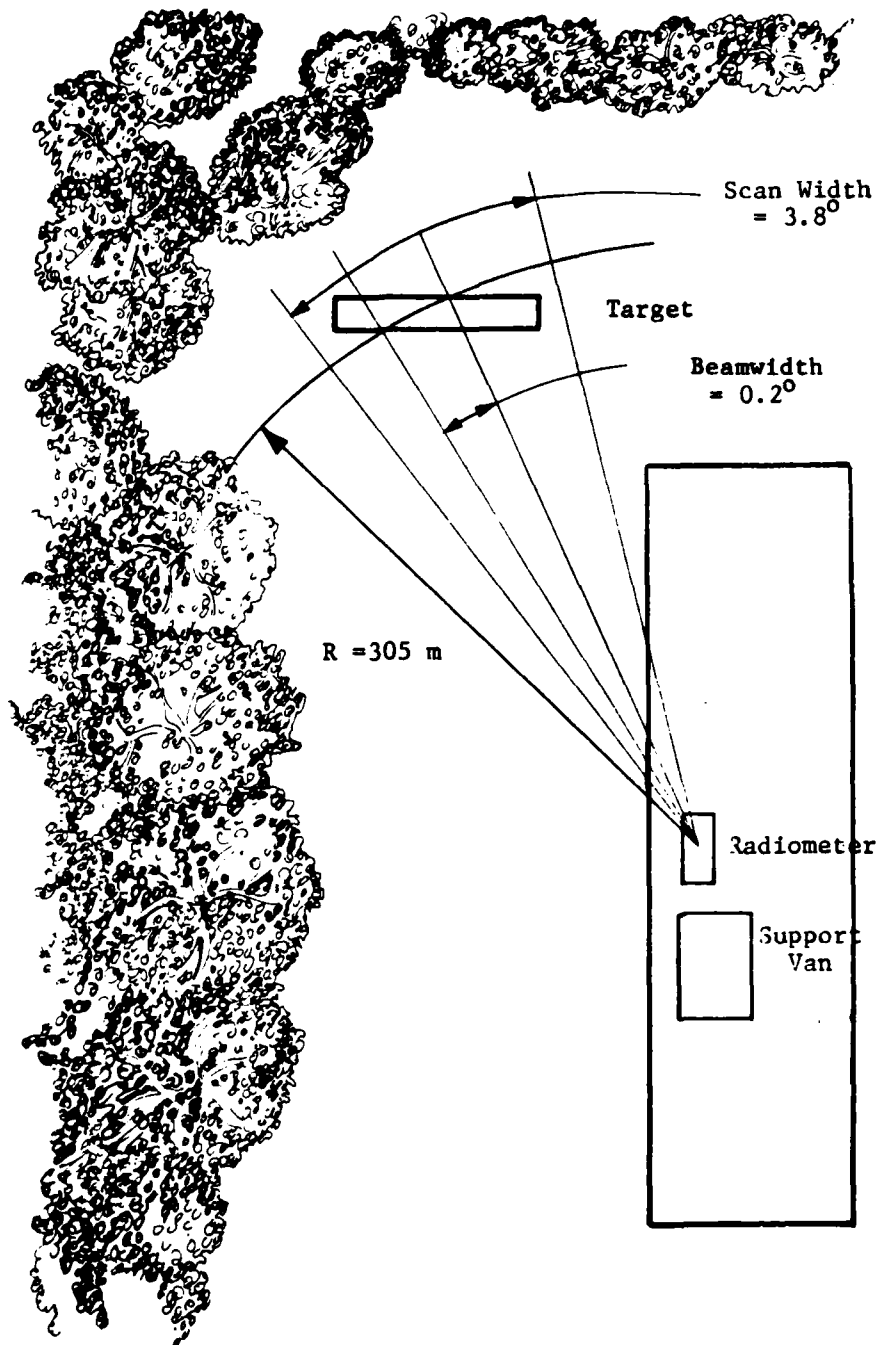


Figure 4. Test Site Geometry

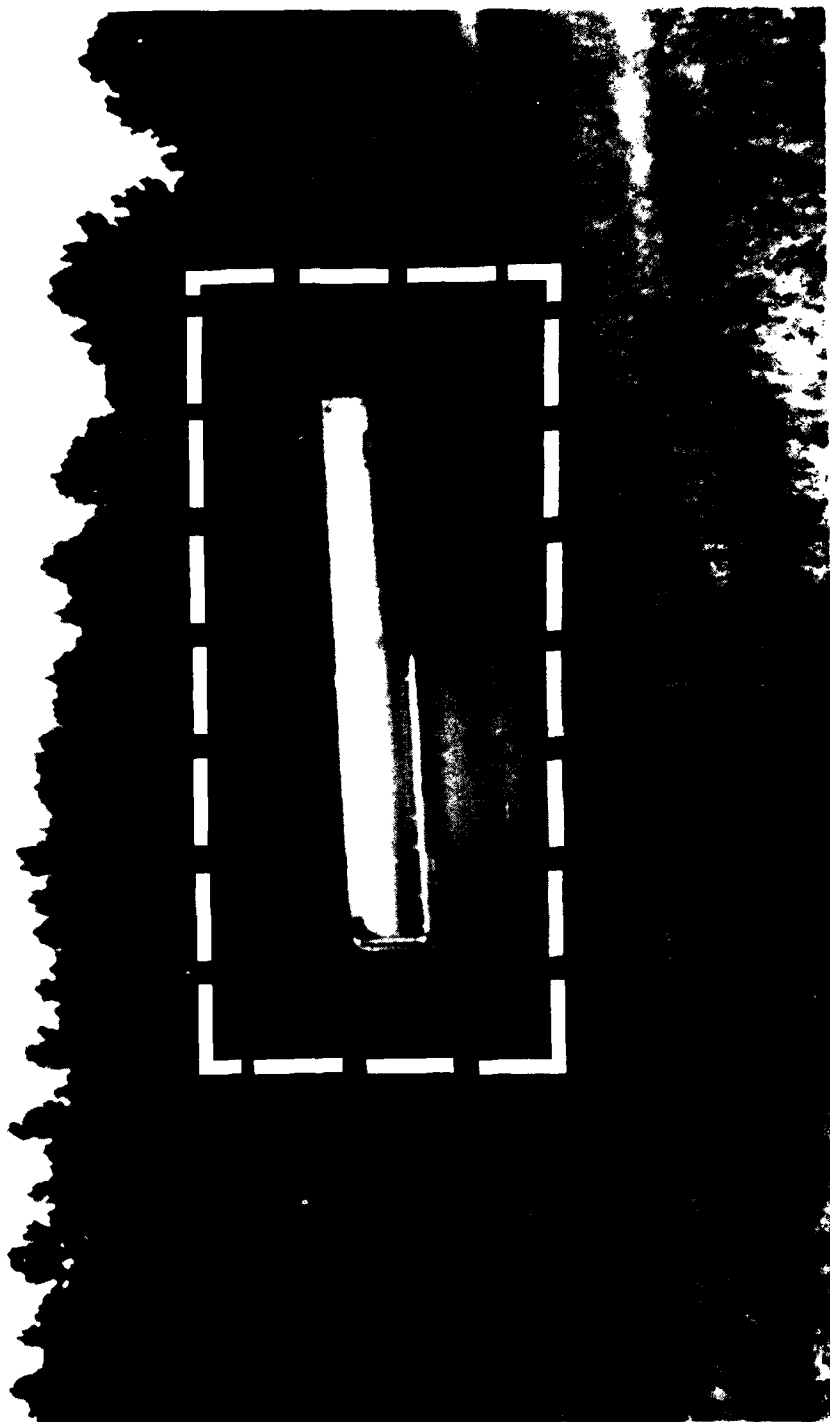


Figure 5. Test Site Photograph

half power beamwidth). In scanning this raster, motion on adjacent scan lines is in opposite directions, i.e., the radiometer scans from left to right on the first scan line, moves down to the next scan line, and then scans from right to left.

### 3.5 Measurements Schedule

The equipment was transported to the measurements site June 18, 1980. The tanker target was delivered June 19, 1980. The tests were conducted from June 19 through June 26. A complete log of activities is given in Appendix A2.

#### 4.0 Data

Much of the data were recorded on strip charts. Both target and calibration data were obtained from these strip charts. The temperatures of the hot and ambient loads were known so the equations from Section 1.3.2 of Appendix A1 were used to find the apparent radiometric temperatures of all other data in that calibration or associated scene. Weather data were recorded separately and associated with specific radiometric data by time and date.

##### 4.1 Data Format

Each scan line of the raster scan is presented on a separate line. The horizontal scale represents angular distance and the vertical scale apparent radiometric temperature. The scan lines were arranged on the area of the target as shown in Figure 6. A nine track digital tape containing a raster scan with both 95 GHz and 220 GHz data was delivered simultaneously with this report. The 95 GHz data were recorded in real time. The 220 GHz data were manually digitized from strip charts and added to the tape at a later time. A complete description of the format of this tape is given in Appendix A4.

##### 4.2 Target Detection

Good target detection data were obtained on June 26, 1980 and are shown in Figure 7. The temperature at the time of this scan was  $28.3^{\circ}\text{C}$  ( $83^{\circ}\text{F}$ ) and the relative humidity was 61%. The dual diode mixer was used with an integration time of 5 seconds yielding  $\Delta T_{\text{min}} = 0.6 \text{ K}$ . The sky temperature was 255 K. On scan line five (which passes through the target as shown in Figure 6) the abrupt temperature change to approximately 6 K below ambient indicates a definite target detection. The scan above the target (scan line 4) and below the target (scan line 6) show warmer temperatures. These results are very close to those anticipated based on the conditions during the tests.

For comparison a 95 GHz digitally recorded image is shown in Figure 8. The sky temperature at 95 GHz was 67 K. Image resolution is somewhat poorer due to the antenna's larger beamwidth at 95 GHz. A digital image of the 220 GHz data in Figure 7 is shown in Figure 9.

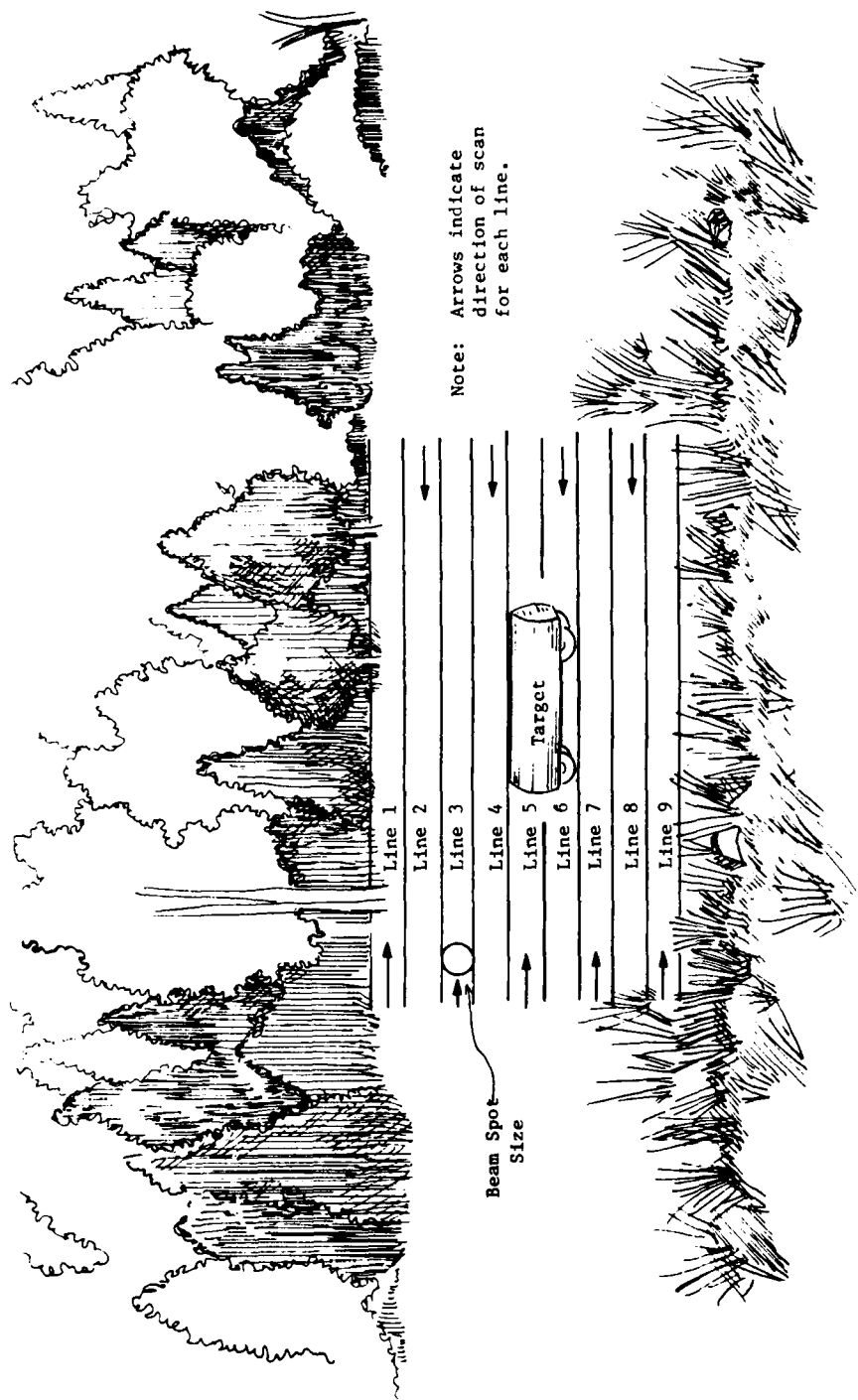


Figure 6. Raster Scan Geometry.

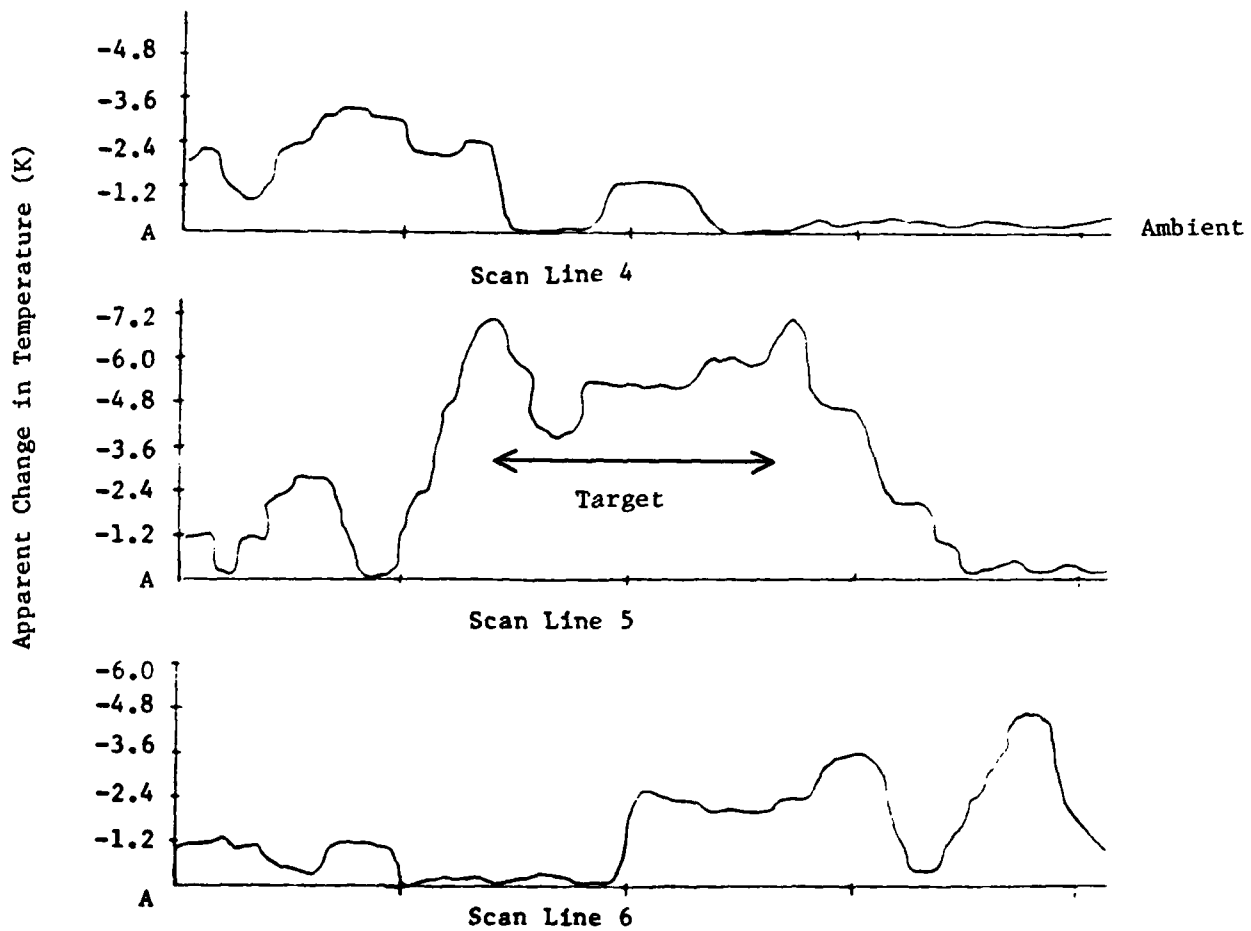


Figure 7. Target Detection Strip Chart.

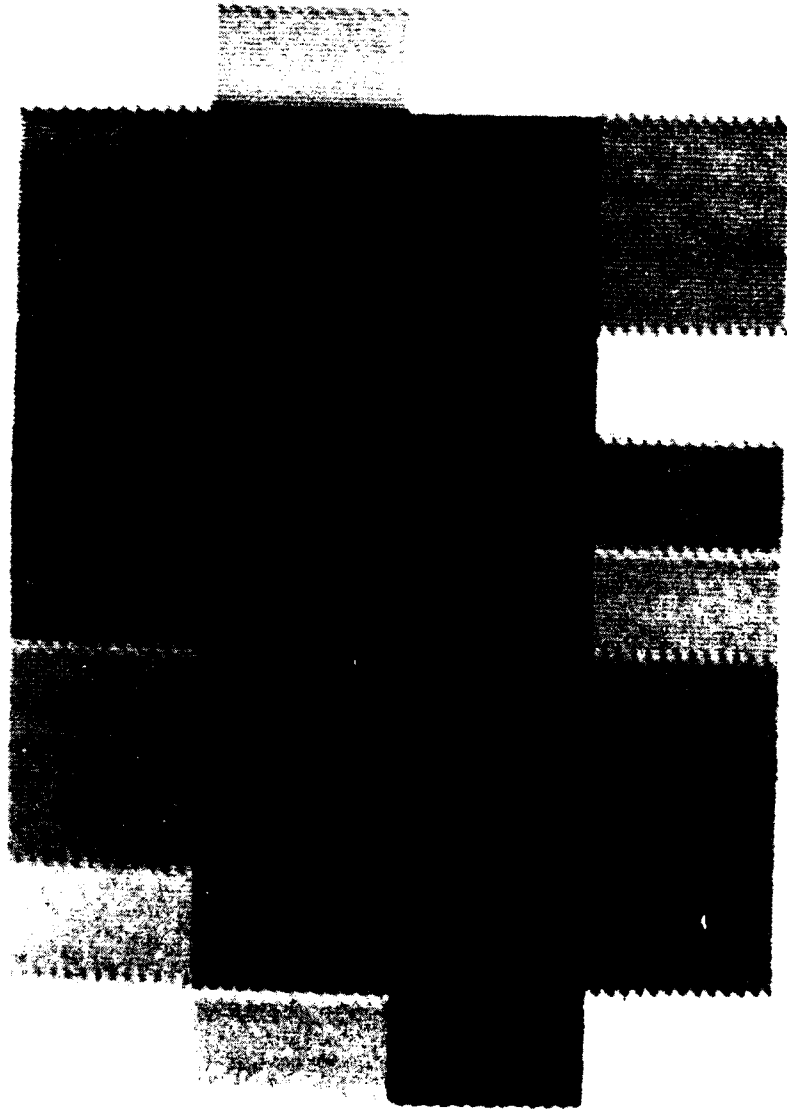


Figure 8. 94 GHz Digital Image

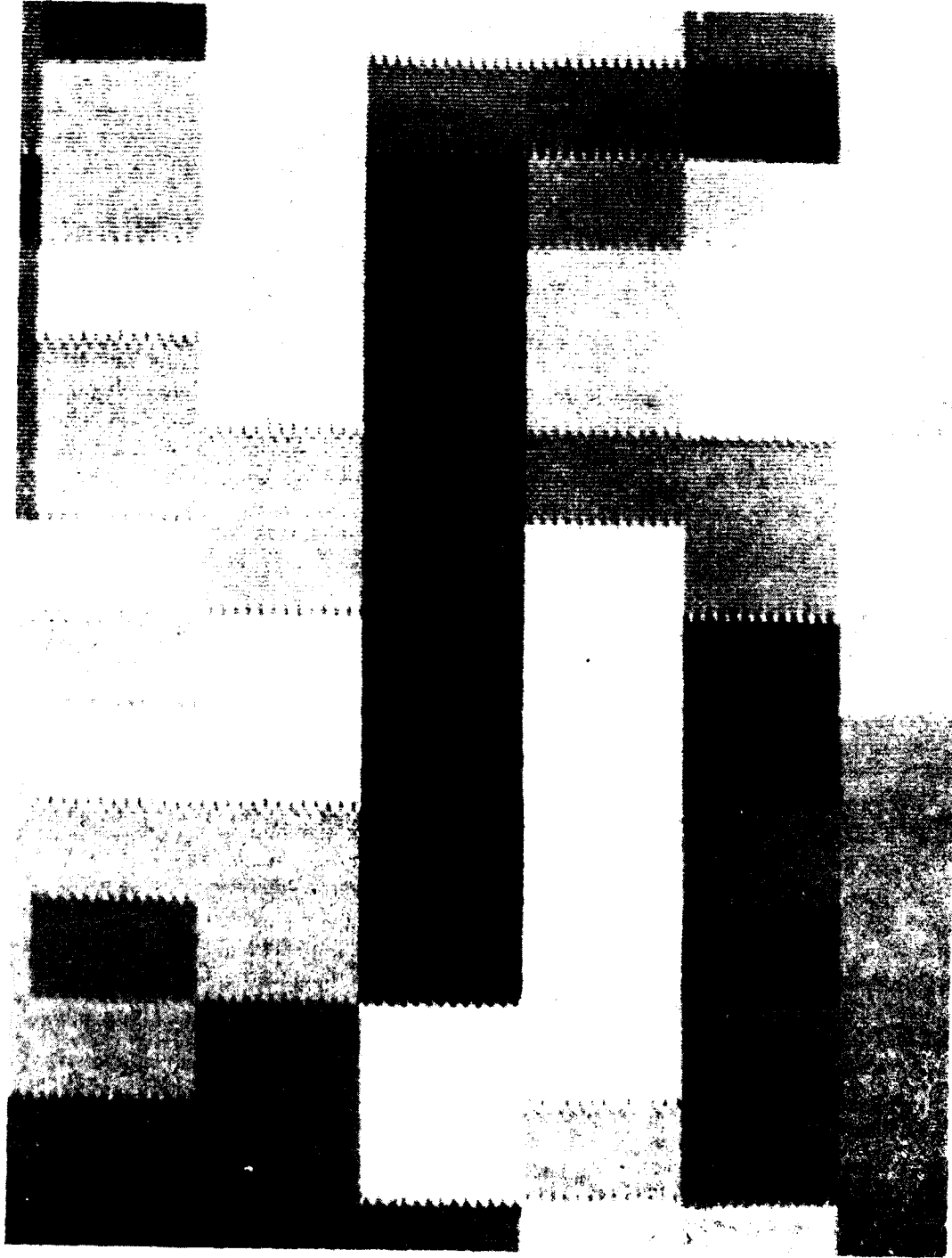


Figure 9. 220 Cliz Digital Image

#### 5.0 Acknowledgment

The authors acknowledge NASA Grant NSG-5012 under which the dual diode subharmonically pumped 220 GHz mixer used in this program was developed. Appreciation is expressed to the U.S. Army personnel at Fort Gillem, Georgia. We would also like to acknowledge the valuable contributions to this project of the following Georgia Tech personnel:

S.M. Halpern, D.S. Zacharias, J.M. Newton and T.D. Semones.

Appendix A1

Detailed Radiometer Description

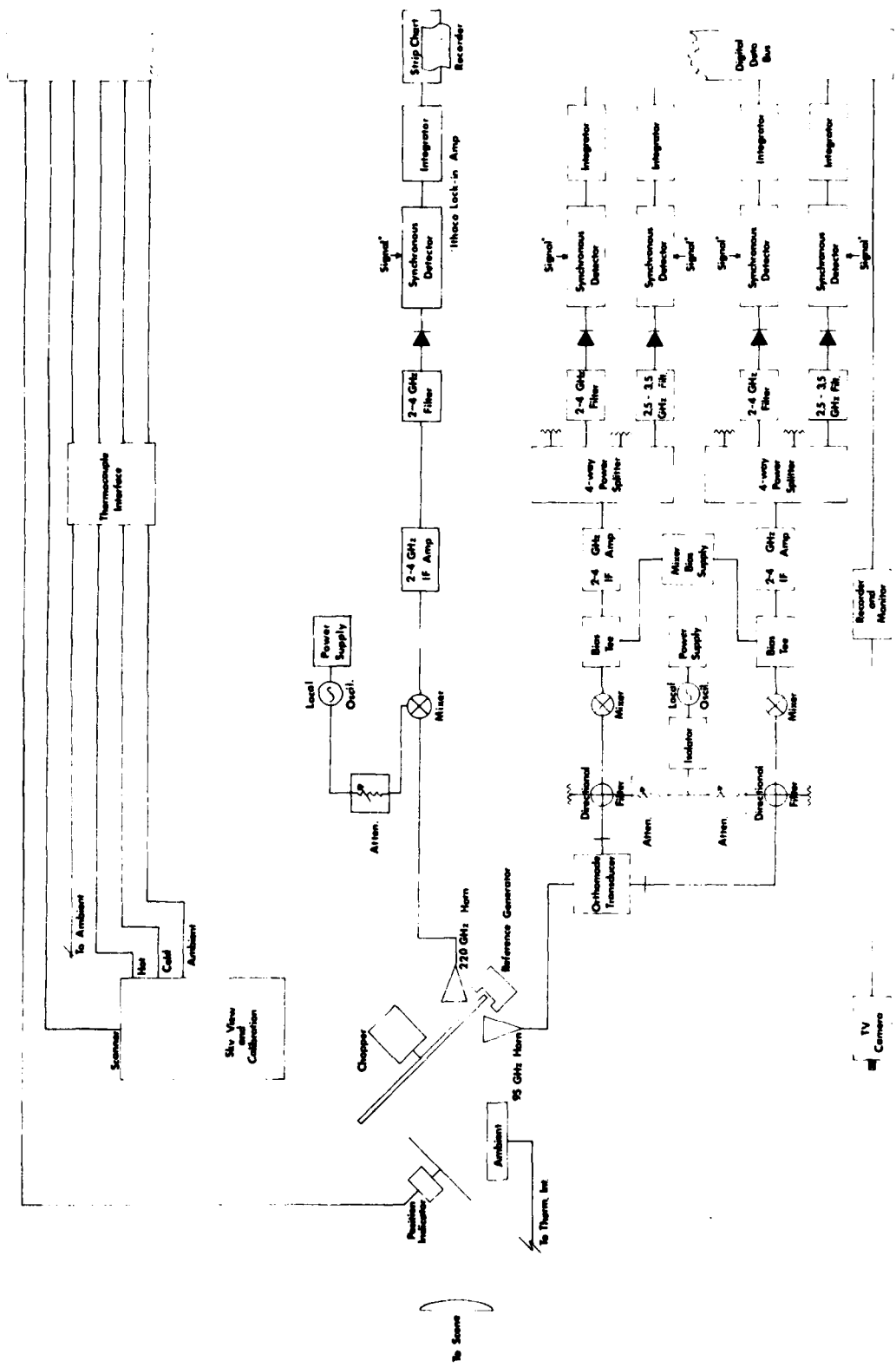
## A1.0 Radiometer Hardware

Figure A1 is a detailed block diagram of the measurement radiometer which uses 220 GHz and 95 GHz RF channels for making the target signature measurements. The radiometer and the support instrumentations consists of the following elements: internal hot/cold load calibration system, 220 GHz RF head (scene and sky viewing), 95 GHz RF head (scene and sky viewing), TV camera unit (scene truth), a rotary platform for the sensors, radiometer receiver (IF amplifiers, filters, square law detectors, synchronous detectors, and integrators), data acquisition system (microcomputer based), and tape recorders (multichannel data and TV). A simplified pictorial diagram of the system is shown in Figure A2. The measurement radiometer provides the following: 1) precise scene resolution, 2) low noise operation for good temperature resolution, 3) adequate stabilization of electronics for good temperature resolution, and 4) good absolute temperature measurement accuracy.

A description of the radiometer follows. The 95 GHz frequency channel operates simultaneously with the 220 GHz channel by using the super chopper (rotating reflective blade) concept. The 220 GHz/95 GHz feed horns receive the signal from the scene (target), sky view, or internal calibration loads as selected by the data acquisition system (DAS).

The feeds are corrugated conical horns. A 6 inch diameter Rexolite lens having a  $f/D$  ratio of 1 is illuminated by the horns.

The lens focuses energy from the horn to a spot 6 inches from the lens so that beam switching may be easily accomplished. The focused beam may be reflected by the small switching reflector into one of the calibration loads or allowed to pass unblocked. The unblocked beam illuminates the 20-inch radiating aperture.



\*Signal from Reference Generator

Figure A1. System Block Diagram

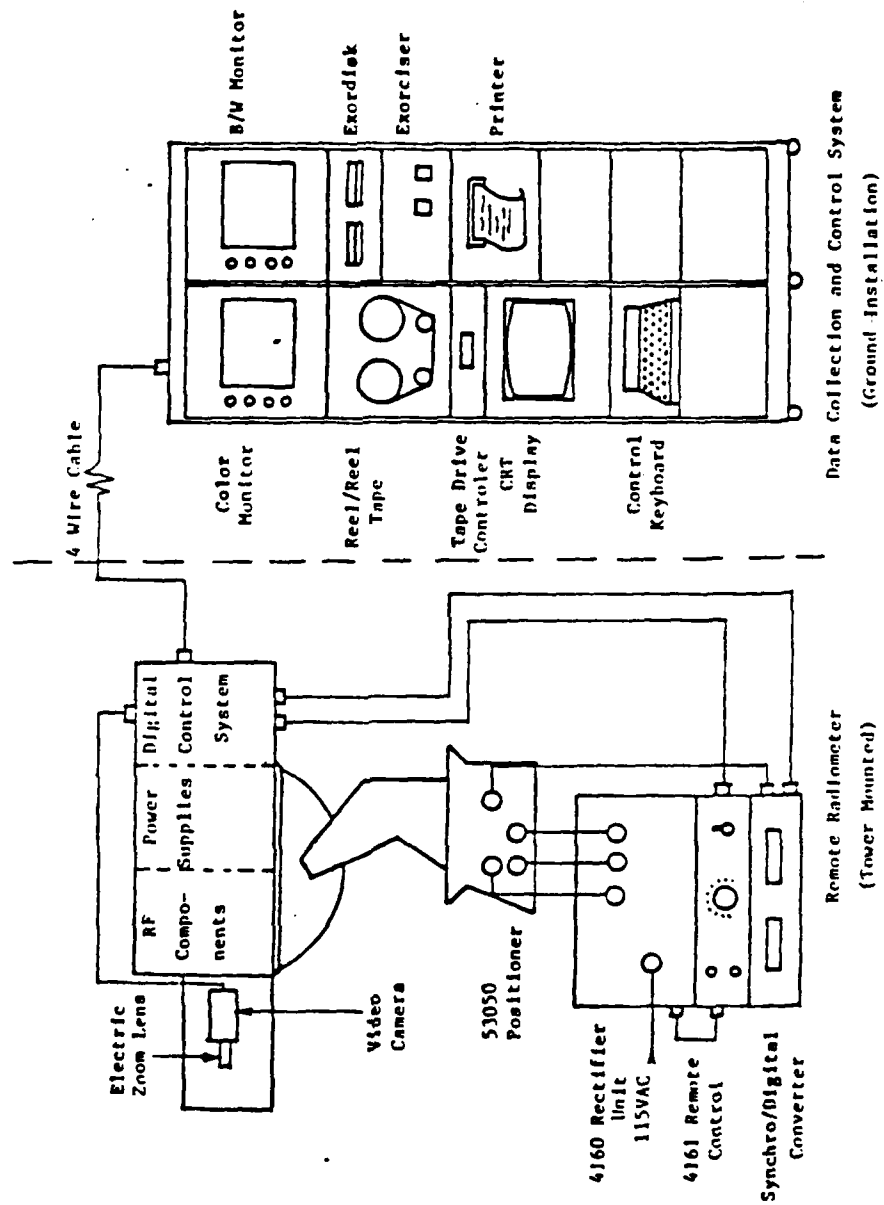


Figure A2. Millimeter-Wave Instrumentation Radiometer.

The 20-inch lens is designed to correct the phase of the incoming RF signal so that it is focused at the correct target range. Adjustments of the focal distance is accomplished by moving the 20-inch lens along the lens/horn axis. The 3 dB beamwidth of this antenna is  $0.44^\circ$  at 95 GHz and  $0.19^\circ$  at 220 GHz.

#### A1.1 95 GHz System

The signal exits via the horizontally and vertically polarized output ports of the orthomode transducer. Each polarized signal is down-converted in a separate mixer to an IF of nominally 2.0 to 4.0 GHz. The local oscillator signal is injected into each mixer using a directional filter.

The IF is split off using a 4-way power divider into two bandpass filters and two termination loads. These bandpass filters provide passbands of 1 GHz and 2 GHz centered on 3 GHz. The two extra ports which are terminated are spare paths for future growth that could be used with different bandpass filters or be used for IF correlation of the H and V channels. Square law detectors follow each bandpass filter as shown. The detected Dicke modulated signal in each channel goes to a phase sensitive detector (PSD) whose input is multiplied by the super chopper reference generator. The reference signal switches the detector output in synchronization with the antenna signal. Thus, the output voltage from the PSD is directly proportional to the scene temperature. The integrator is a low-pass filter having an integration time which is selected to yield an acceptable temperature resolution. All integrator outputs are then routed to the data acquisition system.

#### A1.2 220 GHz System

The 220 GHz signal goes to a subharmonically pumped mixer where it is down-converted to an IF of nominally 2 to 4 GHz. Two mixers were used in this measurement program, a conventional single diode unit harmonic mixer and a two-diode subharmonically pumped unit designed and built by Georgia Tech. The local oscillator signal is supplied by a Varian klystron operating at 109 GHz. It is injected directly into the mixer.

The IF signal is amplified by two Narda amplifiers in series each of which has approximately 35 dB of gain. It is then bandpass filtered to 2 to 4 GHz and detected by a Schottky diode square law detector.

The detected signal then goes to an Ithaco-391A lock-in amplifier. The Ithaco-391A performs the functions of a video amplifier, phase sensitive detector and integrator. The video gain and integration time are adjustable. The integration times used for these tests were typically five seconds with the dual diode mixer and sixteen seconds with the single diode mixer. The output of the lock-in amplifier is a dc voltage proportional to the radiometric temperature of the scene. This signal was routed to a chart recorder.

#### Al.2.1 Single Diode Mixer

The single diode mixer is shown in Figure A3. The local oscillator is fed directly to the diode via a waveguide which intersects perpendicularly with the signal waveguide. There are tuning backshorts in both the signal and local oscillator waveguides. The diode in the mixer was installed and contacted at Georgia Tech.

#### Al.2.2 Dual Diode Mixer

The dual diode mixer is shown in Figure A4. It was originally designed to operate at 183 GHz ( $\pm 11$  GHz) with a 91.5 GHz local oscillator. It is a subharmonic mixer using two antiparallel mounted diodes in the signal waveguide as shown in Figure A4. The LO is injected through a suspended substrate stripline low pass filter after being launched onto the substrate with a waveguide to stripline transition. The IF filter blocks the LO but passes the IF frequencies (0.4 - 10 GHz) to the IF port. Tunable backshorts are used in both the LO and signal waveguides to tune the mixer. This mixer operates with about 10 to 20 mW of LO power.

### Al.3 System Calibration

#### Al.3.1 Internal Load Calibration System

The RF sensor portion of the measurement radiometer is shown in Figure A5. The radiometer utilizes a rotating reflective blade chopper (super chopper). The super chopper concept allows the simultaneous sharing of the chopper, the antenna and the reference loads



Figure A3. Single Diode Mixer

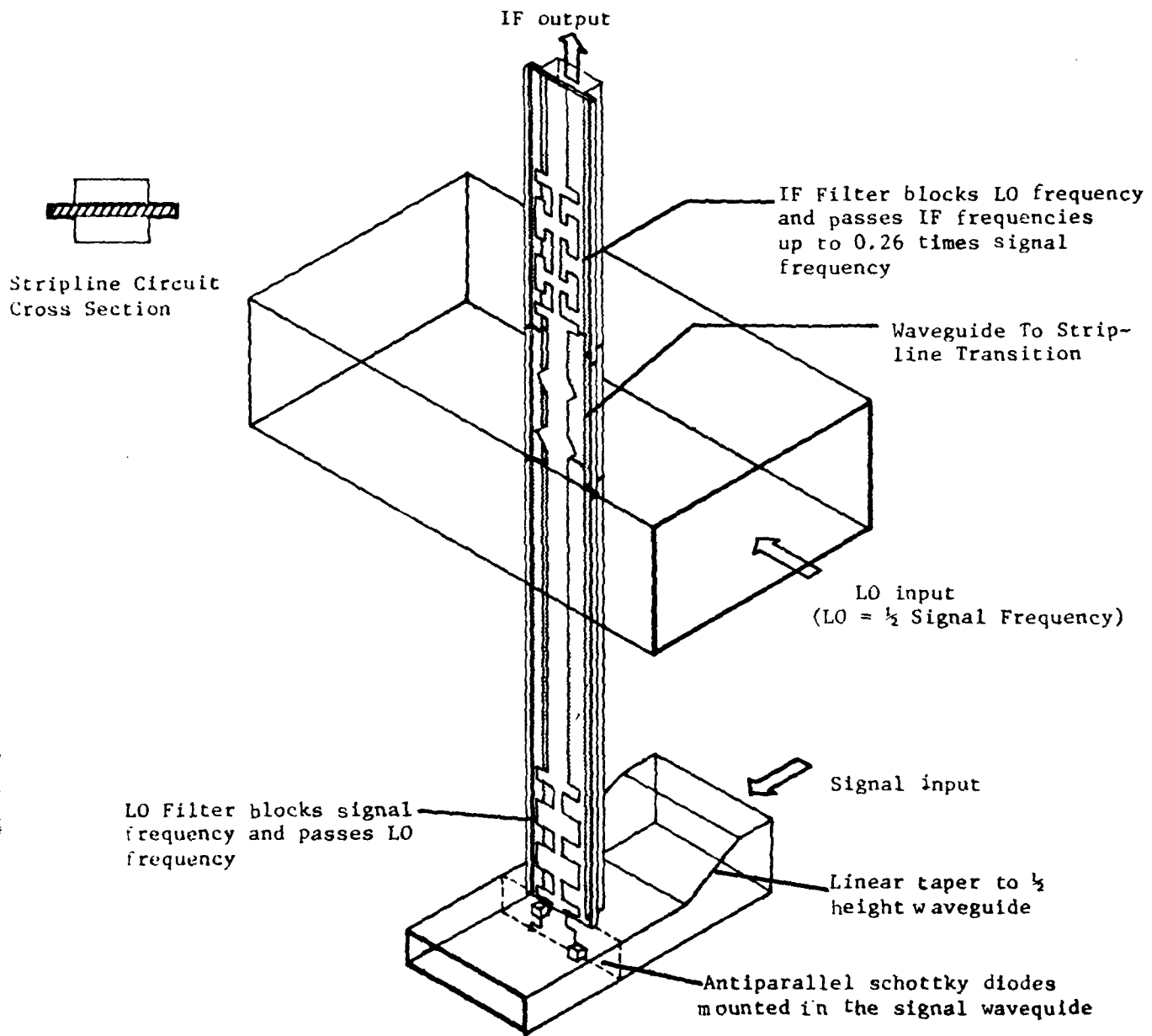


Figure A4. Functional Schematic of Subharmonic Mixer.

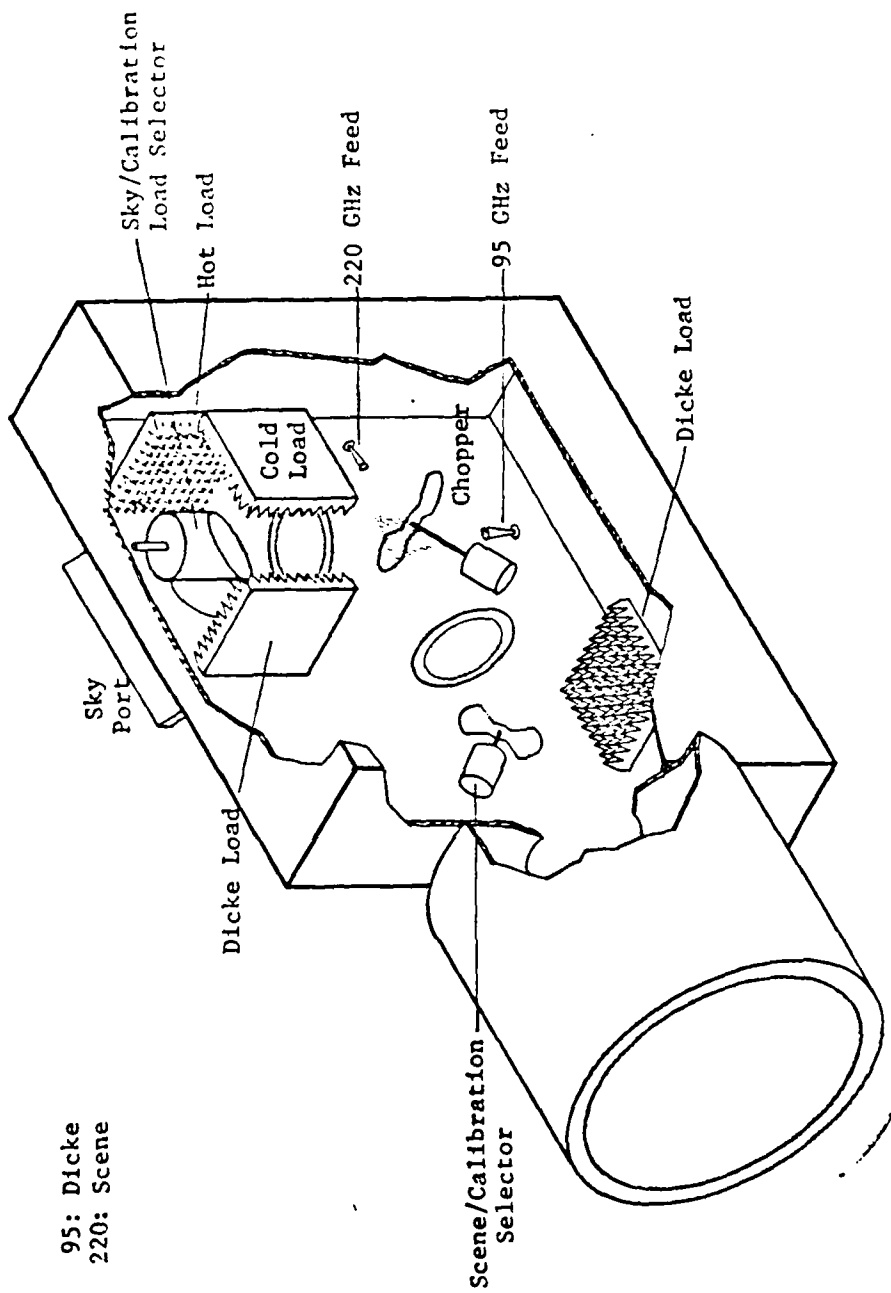


Figure A5. RF Portion of Radiometer.

by two different feed antennas thus permitting simultaneous operation at 95 GHz and at 220 GHz. The feed horn antenna alternately views the upper and lower chamber ports as the chopper blade passes in front of the antenna.

One of these ports views an ambient temperature load used as the Dicke reference while the other views either a scene with an unknown temperature (data taking) or a known temperature reference load (calibration). During data taking the lower port views the scene through the large lens while the upper port views the Dicke reference load. For calibration the lower port is reflected to view the second Dicke reference load. The upper port successively views the sky (via the sky reflector), the hot load, the cold load, and the upper Dicke reference load. Both the upper and lower reflectors are positioned by stepper motors under computer control.

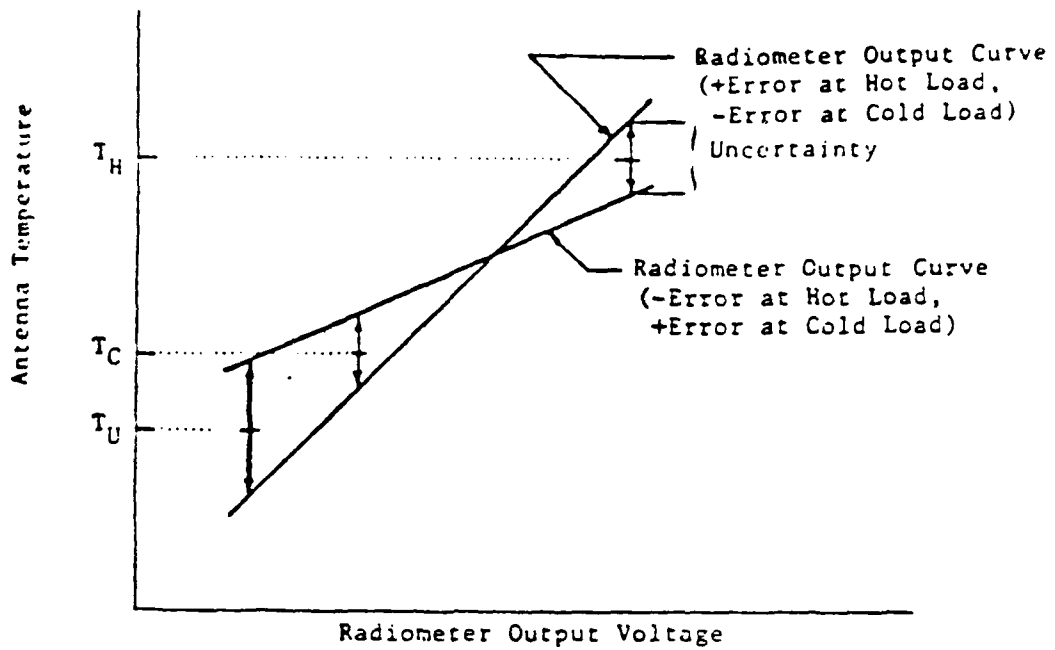
The loads consist of pyramids made with a ferrite epoxy absorbing material adequate for both polarizations. The pyramids are cut at the Brewster angle to minimize reflections. The hot load is heated with heating elements and the cold load is cooled with liquid nitrogen. The cold load temperature is monitored by a thermocouple. All other load temperatures are monitored by thermistors routed through a multiplexor to the computer. Thermistors handled by the same multiplexor monitor the operating temperature of several major RF components and the large lens.

#### Al.3.2 Calibration Equations

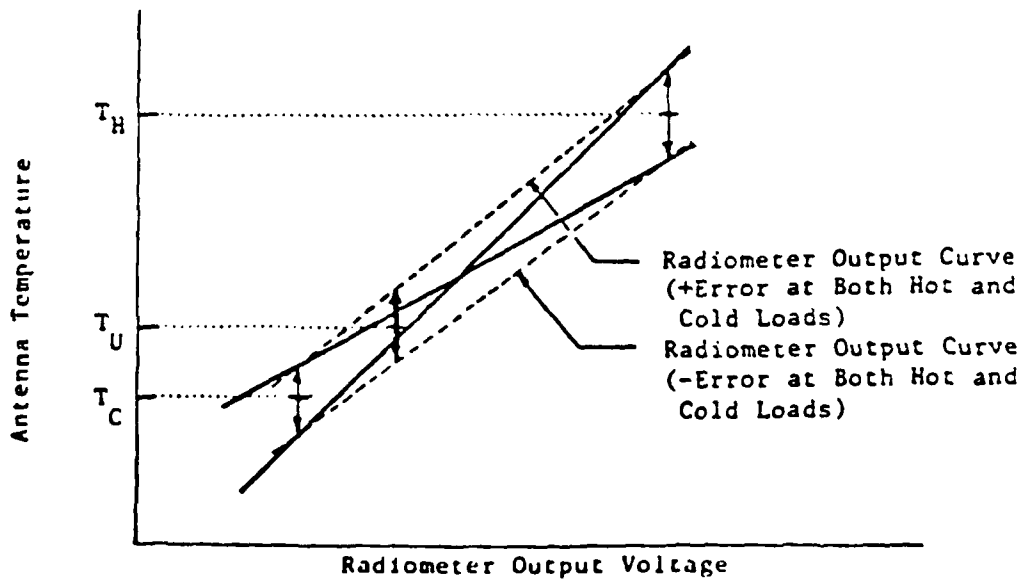
Radiometer calibration requires fitting the point-slope equation of a line to the calibration data. The antenna temperature of a radiometer is thus,

$$T_A = sV_o + O_f.$$

The use of hot and cold calibration loads to calibrate the radiometer involves a trade-off of absolute accuracy, measurement uncertainty and the actual temperatures of the hot and cold loads and the load temperatures relative to an unknown temperature. Figure A6 shows aspects of this situation. Two cases are given: one for the case



a.  $T_{\text{UNKNOWN}}$  Outside of the Hot and Cold Load Temperature Range.



b.  $T_{\text{UNKNOWN}}$  Between Hot and Cold Temperature.

Figure A6. Calibration Load Temperature and Unknown Load Temperature Relationships.

where the unknown temperature is outside the temperature range between the hot and cold loads and the second case where the unknown temperature is in the temperature range between the hot and cold load. The graphs generally show that the uncertainty associated with the unknown temperature is lower when this temperature falls between the hot and cold load temperatures.

The precise relationships are shown in Figure A7. For the case where the unknown temperature is outside the temperature region between the hot and cold loads, the relationship for the temperature uncertainty is

$$\Delta T_U = \Delta T_X \left[ 1 + 2 \left( \frac{T_C - T_U}{T_H - T_C} \right) \right]$$

where

$T_U$  = Temperature uncertainty for the unknown scene temperature

$T_U$  = Unknown scene temperature

$T_X$  = Radiometer measurement uncertainty

$\Delta T_X = \Delta T_{\min} + \Delta T_{\text{THER}}$

$\Delta T_{\min}$  = Radiometer minimum detectable temperature

$\Delta T_{\text{THER}}$  = Uncertainty of the thermistor output used to measure the calibration load temperature

$T_H$  = Hot load temperature

$T_C$  = Cold load temperature

For the case where the unknown temperature is between the hot and cold loads  $T_U = T_X$ .

To illustrate the trade-off, the following parameters will be used:

$T_H = 340\text{K}$

$T_C = 290\text{K}, 100\text{K}$

$\Delta T_{\text{THER}} = 0.1\text{K}$

$\Delta T_{\min} = 1.0\text{K}$

$\Delta T_X = 1.1\text{K}$

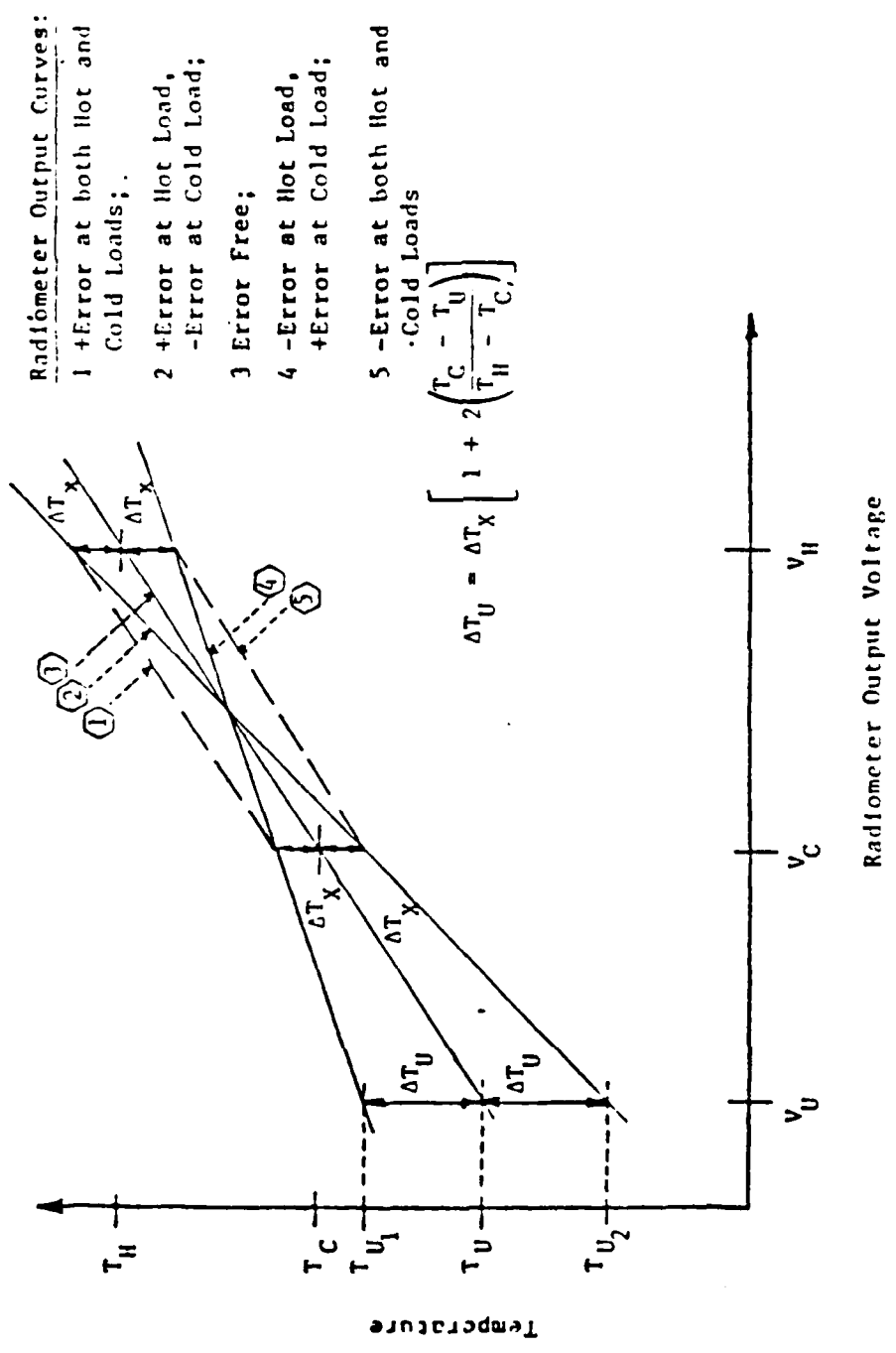


Figure A7. Error Limits in the Radiometer Output Functions.

The hot and cold load temperatures above are easily obtained. The thermistor error is that of a typical thermoliner device and the minimum detectable temperature is assumed as 1 K. Figure A8 plots the measurement uncertainty for this case. It can be seen that for the low temperature range plotted, the measurement uncertainty exceeds  $\pm 10$  K when the unknown scene temperature is about 40 K with the 340 K hot load. Since lower scene temperatures were anticipated and the insulating foam used places an upper limit of 340 K on the hot load temperature, a liquid nitrogen cooled cold load was used. The combination of a 340 K hot load and a 100 K cold load gives acceptable measurement uncertainties throughout the entire range of expected scene temperatures.

#### Al.4 Auxillary Equipment

##### Al.4.1. Antenna Positioner and Controls

A Scientific Atlanta Model 54050 antenna positioner is used to rotate the radiometer during the tests. The 54050 positioner is an elevation-over-azimuth unit that allows the measurement of true vertical and horizontal polarization. The alternate choice for this program was the azimuth-over-elevation positioner that does not allow the unambiguous measurement of the polarizations.

The positioner is controlled by computer via a Georgia Tech built interface. The computer sends an axis selection, a direction selection, and a speed voltage to the interface which passes them along to the positioner. Angle information is obtained in the following manner. Each axis of the positioner has two synchro position indicators (a 1:1 and a 36:1). The computer-positioner interface converts the synchro outputs to binary coded decimal angles and passes them to the computer. The angle readouts are 0.01 degrees and the positioner is positioned to  $0.10 + 0.09/-0.00$  degree accuracy.

##### Al.4.2 Television Camera

A television camera is used to provide a record of the scene imaged by the radiometer and to setup the limits of scan patterns. The camera is initially aligned with the center of the field-of-view of the radiometer antenna. The camera mount provides a rigid support to

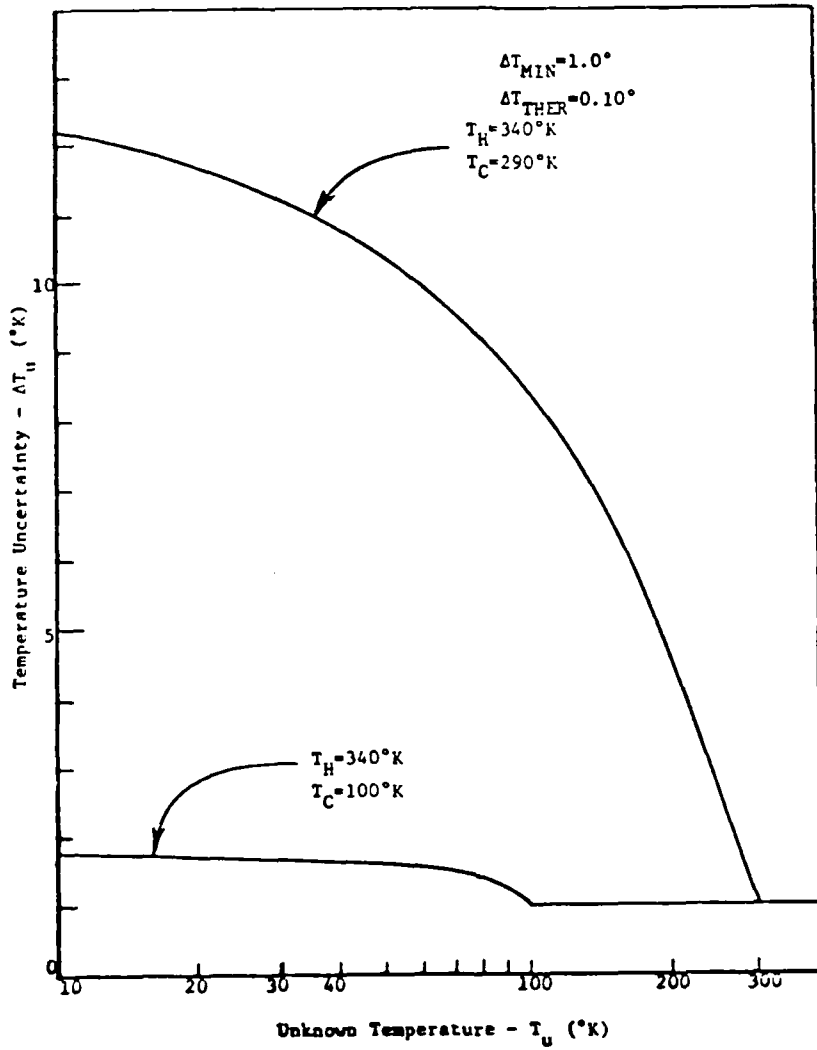


Figure A8. Measurement Uncertainty vs. Unknown Temperature

maintain this initial alignment. This alignment is done with a reflector mounted near the target which is located radiometrically and optically to provide a camera-radiometer alignment.

The television camera is equipped with a zoom lens which has remotely controllable zoom, focus and iris opening. These are controlled from the operator's console via the computer. The camera field-of-view can thus be matched to the radiometer field of view and the iris can be adjusted to cope with changing light conditions.

Appendix A2

Measurements Log

### Measurements Log

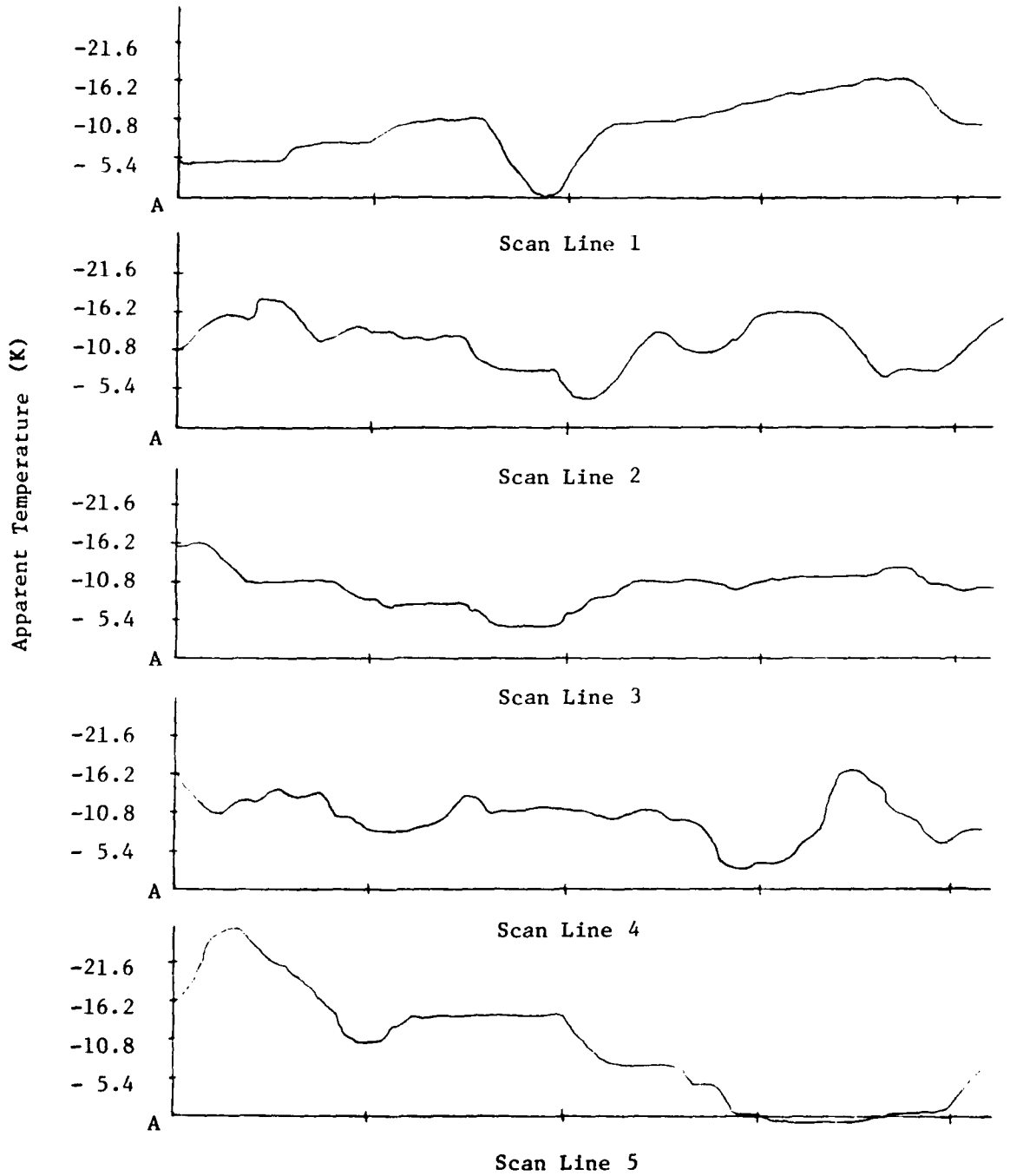
<u>Date</u>	<u>Comments</u>
6-18-80	Equipment taken to site. Preliminary equipment checkout performed.
6-19-80	Target delivered. First 220 GHz data run. Lens loss and sky temperature measurements.
6-20-80	Single diode mixer used mainly. First target scan done. No target detections.
6-21-80	Rain. No data taken.
6-22-80	Rain in morning. Prepared for data taking in evening.
6-23-80	Weather conditions poor. No activities.
6-24-80	Dual diode mixer not working. No target detection possible with weather conditions and single diode mixer performance.
6-25-80	Sky temperatures very high. No target detections.
6-26-80	Sky temperatures moderate. Many scans taken. Target detection data obtained.
6-27-80	Tests over. Equipment brought back to Georgia Tech.

Appendix A3

Target Scans

### A3.1 Data Overview

The data presented in this appendix were taken from strip chart recordings. Each scan line in the raster is presented on a separate line. The horizontal scale represents angular distance and the vertical scale represents apparent radiometric temperature. These temperatures are not corrected for lens loss. The base line is ambient. Each raster consists of nine scan lines.



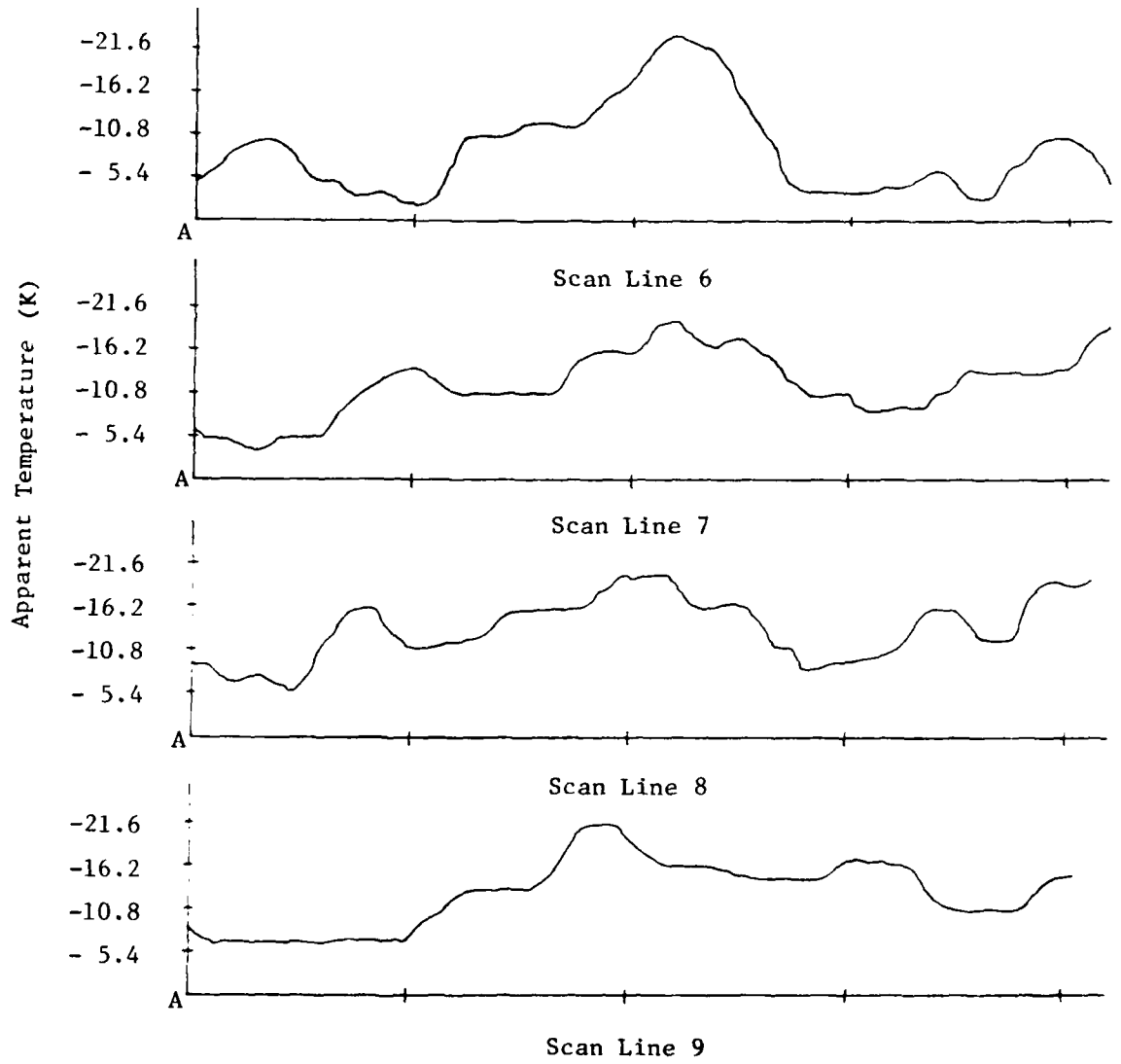
Date: 6-20-80

$T_{\text{sky}}$ : 240 K

Time: 6:30

$\Delta T_{\text{min}}$ : 5.4 K

Figure A9. Raster Scan #1

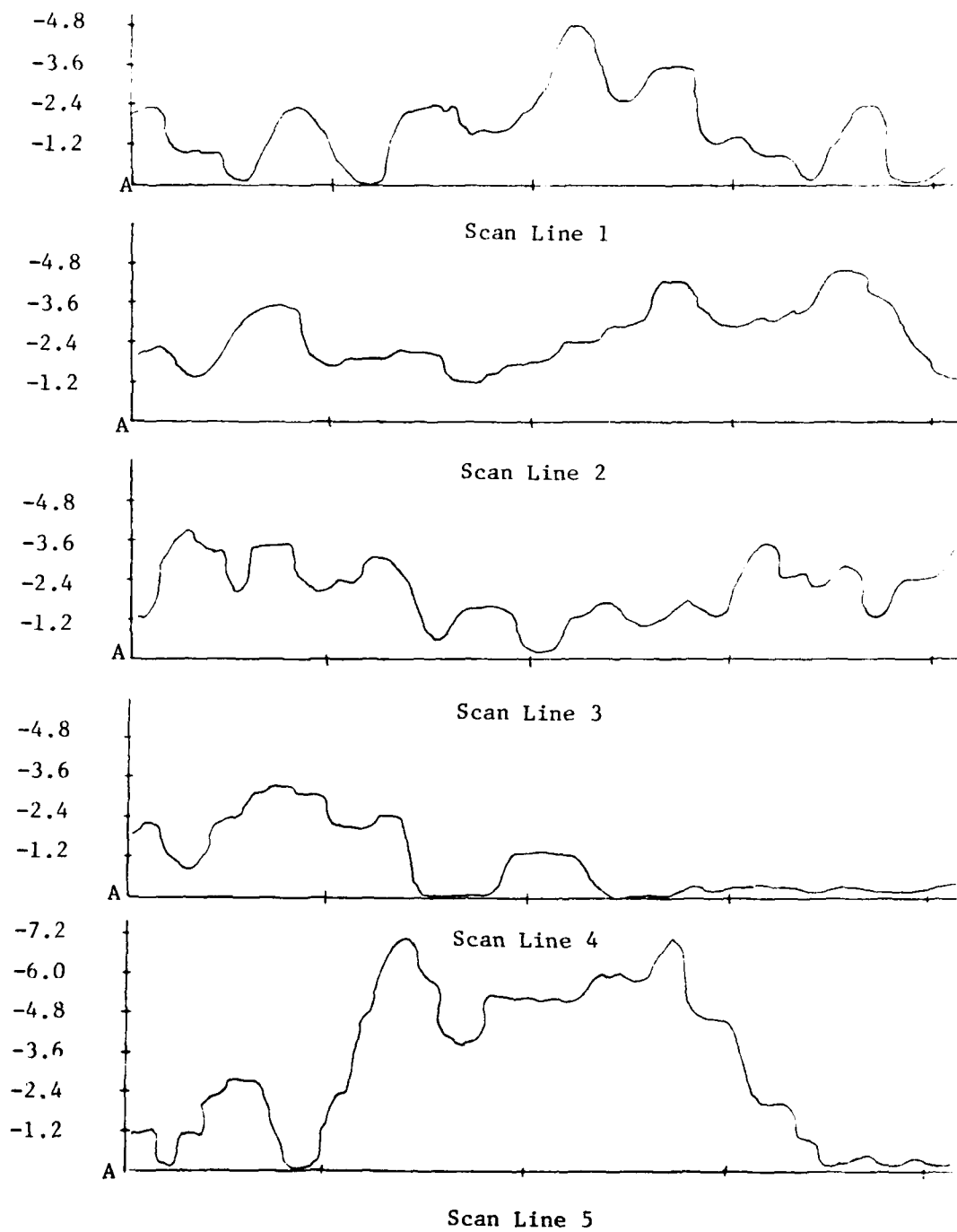


Date: 6-20-80  
 Time: 6:30pm  
 $\Delta T_{\min}$ : 5.4 K

$T_{\text{sky}}$ : 240 K

Figure A10. Raster Scan #1 (cont'd.)

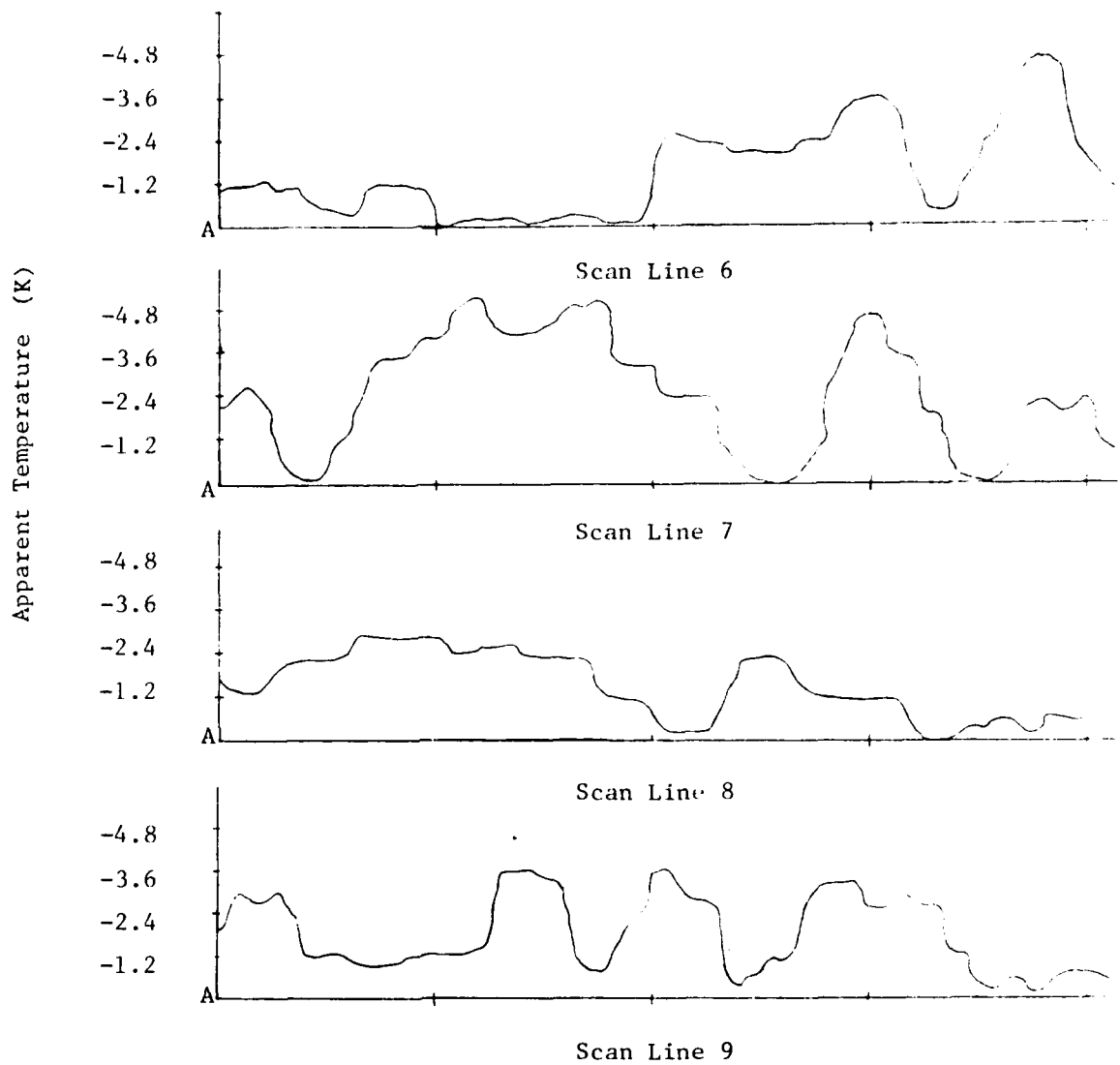
Apparent Temperature (K)



Date: 6-26-80  
Time: 9:30am  
 $\Delta T_{\min}$ : 0.6 K

$T_{\text{sky}}$ : 255 K

Figure A11. Raster Scan #2

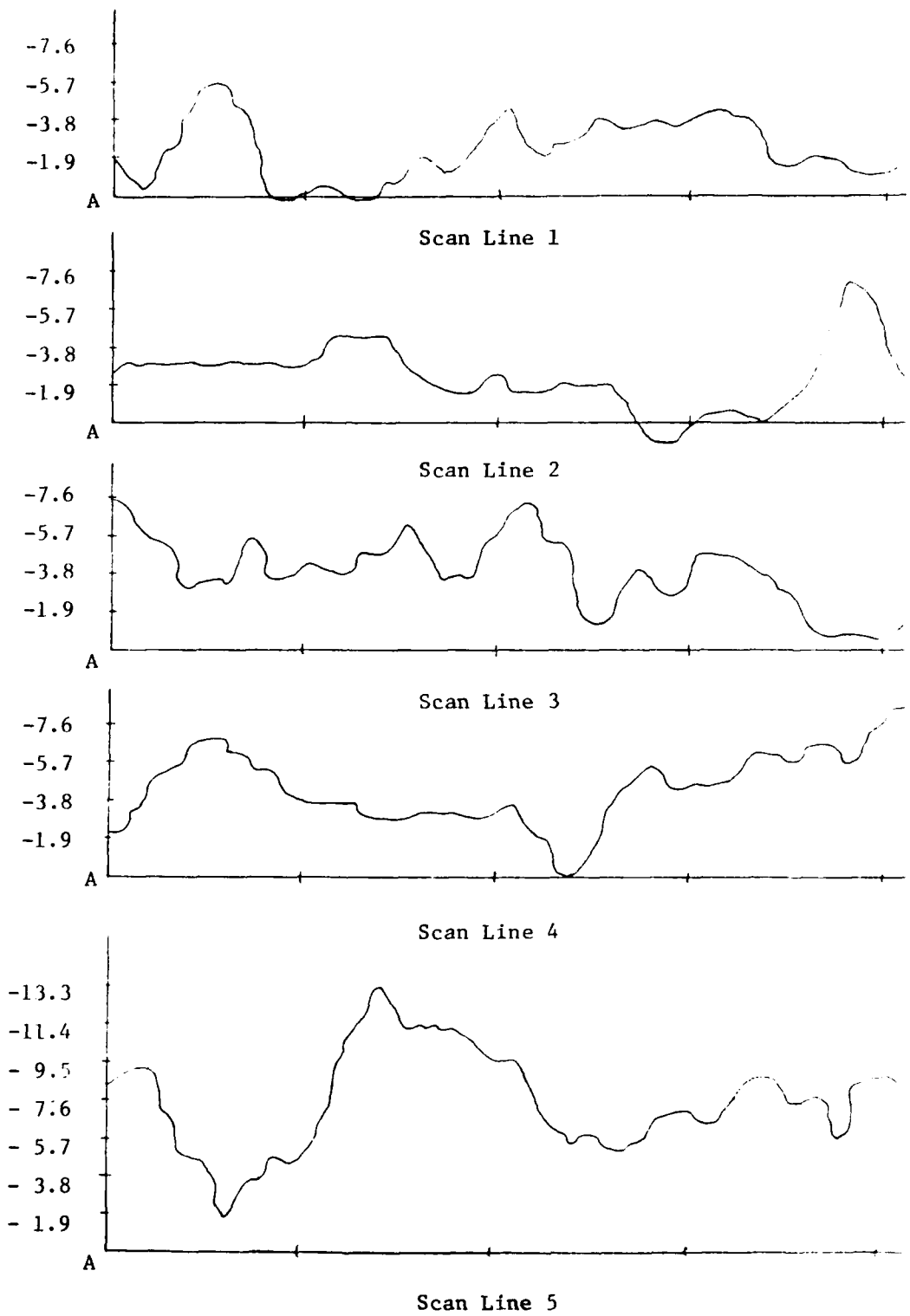


Date: 6-26-80  
 Time: 9:30am  
 $\Delta T_{\min}$ : 0.6 K

$T_{\text{sky}}$ : 255 K

Figure A12. Raster Scan #2 (cont'd.)

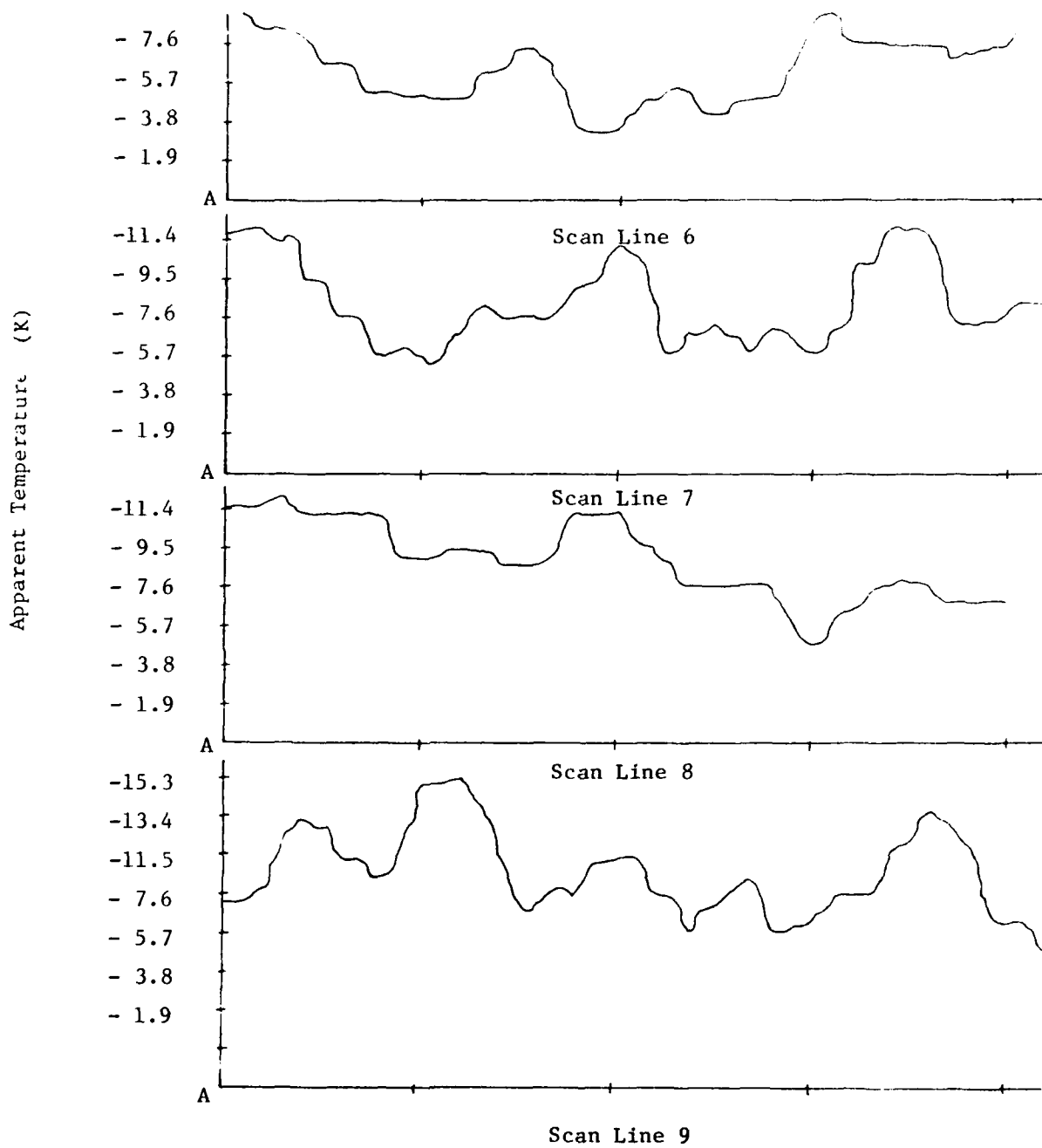
Apparent Temperature (K)



Date: 6-26-80  
Time: 7:00pm  
 $\Delta T_{\min}$ : 0.8 K

$T_{\text{sky}}$ : 241 K

Figure A13. Raster Scan #3



Date: 6-26-80  
 Time: 7:00pm  
 $\Delta T_{\min}$ : 0.8 K

$T_{\text{sky}}$ : 241 K

Figure A14. Raster Scan #3 (cont'd.)

Appendix A4

Data Tape Format

## TAPE FORMAT

The tapes produced by the DCP contain no label record and are often referred to as "unlabeled" tapes in IBM systems. The logical group of records utilized to record video and radiometric data in this system is referred to as a "scene". Each scene can consist of up to 58 records. Scenes are separated from each other by an EOF mark. Two EOF marks are recorded after the last scene on a tape.

### a. Header Record

The first record in each scene contains ASCII data relating to the time, date, target characteristics, and other operator inputs peculiar to a particular scene. Each byte in the record represents a standard ASCII character with the most significant bit set to zero. Each line of header information may contain a maximum of 80 characters and is terminated by ASCII carriage return and line feed characters. The ASCII EOT character (04) is used to denote the end of header data. All 1024 bytes of the header record may not be used. The last nine bytes of the header record contain the ASCII string "TVPICTURE" denoting the start of video data. Table A1 lists the information fields contained in the header.

### b. Video Image

Immediately following the header record are 30 records which contain data from the video camera, referred to as an "image". The image is arranged as 240 lines of 256 pixels. Each pixel is defined by one of 16 gray scale codes having bit patterns ranging from 0000 (black), 0001, 0010, 0011, 0100, etc. to 1111 (white). Since a pixel is defined by four bits, the image is packed so that each byte represents two pixels. There are 128 bytes used per line, or 30,720 bytes per image. The byte numbers correspond with a position on the screen as shown in Figure A15.

Table A1

Header Information

Item

- 1) ##### (run number)
- 2) GEORGIA TECH MMW PASSIVE TARGET SIGNATURE MEASUREMENTS  
RADIOMETER VERSION #.#
- 3) RUN NUMBER = #####
- 4) DATE AND TIME = (DDMMYYXXXX)#####
- 5) PERCENT CLOUD COVER = ###
- 6) GROUND CONDITION = from Ø - 72 alphanumeric characters
- 7) TEMPERATURE IN DEGREES C = ###
- 8) PERCENT HUMIDITY = ###
- 9) TARGET TYPE = ###
- 10) ADDITIONAL COMMENT = from Ø - 72 alphanumeric characters
- 11) NOMINAL DEPRESSION ANGLE = ###
- 12) TARGET ASPECT ANGLE = ###
- 13) TARGET RANGE = ###
- 14) TØ = ###.# (target centroid azimuth)
- 15) AØ = ###.# (target centroid elevation)
- 16) TCT = ###.# (top center azimuth)
- 17) TCP = ###.# (top center elevation)
- 18) CLT = ###.# (center left azimuth)
- 19) CLP = ###.# (center left elevation)

Notes:

- 1) There is a carriage return and linefeed recorded between items and an end of transmission (EOT) recorded after the final item.
- 2) All information is in ASCII.
- 3) The remainder of the header block after the EOT is filled with nulls except for the last 9 spaces which are the marker "TVPICTURE".
- 4) All numbers are decimal.



### c. Radiometric Data

Data from the eight radiometer channels along with calibration information begin in record 32 of each scene. These records contain both calibration and radiometric image data. Depending on an operator selected option there will be either two, three, or five calibrations per image. A calibration will always precede the first scan line and follow the last line. If option 2 is selected, (three calibrations), an additional calibration will occur after scan line 17. Option 3 (five calibrations) will place calibrations after scan lines 9, 17, 25, and 33, and before the first scan line. Option 1 (two calibrations) will be used unless drift problems within a scene are encountered. The locations of calibration and image data can be discerned by searching the tape for the ASCII event markers described below. Since the number of pixels per line, lines per image, and number of calibrations per scene are variable depending on target depression angle, size, and operator option, the exact location of any data following the video image must be located by searching for the corresponding ASCII event marker (ICALIB, ROW01, etc.)

#### (1) Calibration Data

The calibration data block consists of various physical load temperatures measured by thermistors within the radiometer, and the radiometer output voltages obtained when viewing the internal calibration loads and the sky port. All calibration blocks always contain 124 bytes and are immediately preceded by an ASCII event marker such as "ICALIB" (Initial Calibration) or "CALIB33 (Calibration after Row 33).

Table A2 lists the breakdown of data within the calibration block. Note that all binary data are in a 12 bit format in two bytes with the most significant four bits always equal to zero. Each 12 bit number represents a voltage between 0 and 10 volts and is linearly related to a physical parameter such as temperature by the appropriate equation in Table A3.

Table A2. Calibration Data Block Format

Byte No.	Data
1-16	Radiometer output from sky port channels 0 - 7
17-32	Radiometer output from hot load channels 0 - 7
33-48	Radiometer output from cold load channels 0 - 7
49-64	Radiometer output from Dicke load channels 0 - 7
65-66	Hot load thermistor voltage
67-68	Dicke load #1 thermistor voltage
69-70	Dicke load #2 thermistor voltage
71-72	35 GHz Gunn thermistor voltage
73-74	95 GHz Gunn #1 thermistor voltage
75-76	95 GHz Gunn #2 thermistor voltage
77-78	Large lens thermistor voltage
79-80	Wet bulb thermistor voltage
81-82	Dry bulb thermistor voltage
83-84	Box interior thermistor voltage
85-86	35 GHz mixer #1 thermistor voltage
87-88	35 GHz mixer #2 thermistor voltage
89-90	95 GHz mixer #1 thermistor voltage
91-92	95 GHz mixer #2 thermistor voltage
93-94	Spare #1 thermistor voltage
95-96	Spare #2 thermistor voltage
97-112	Radiometer output from Dicke load channels 0 - 7
113-114	Mixer bias from 35 GHz mixer #1
115-116	Mixer bias from 35 GHz mixer #2
117-118	Mixer bias from 95 GHz mixer #1
119-120	Mixer bias from 95 GHz mixer #2
121-122	Cold load thermocouple voltage
123-124	Spare A/D channel

Table A3. Calibration Equations

(1) All thermistors:

$$T(^{\circ}\text{C}) = 100 \text{ deg} - 10 \text{ deg/volt} (V_T \times 0.002442 \text{ volts/count})$$

where  $V_T$  = thermistor binary voltage ( $\emptyset$  - 4095)

(2) Cold load thermocouple:

a)  $T(^{\circ}\text{C}) = 100 \text{ deg/volt} (V_T \times 0.002442) - 200 \text{ deg}$

b)  $T(^{\circ}\text{C}) = (-25) \text{ deg/volt} (V_T \times 0.002442) + 50 \text{ deg}$

(3) Radiometer brightness temperature:

$$T_R (\text{K}) = T_H + \left( \frac{T_H - T_C}{V_H - V_C} \right) (V_R - V_H) + 273$$

where  $T_H$  = hot load temperature in  $^{\circ}\text{C}$

$T_C$  = cold load temperature in  $^{\circ}\text{C}$

$V_H$  = hot load radiometer output in volts

$V_C$  = cold load radiometer output in volts

$$V_H = .002442 \times V_{\text{HBinary}}$$

$$V_C = .002442 \times V_{\text{CBinary}}$$

$V_R$  = radiometer voltage from scene in volts

(4) True Scene Radiometric Temperature

$$T_S = L (T_M - T_L) + T_L$$

where  $T_S$  = True scene radiometric temperature

$T_M$  = Measured scene radiometric temperature

$T_L$  = Lens temperature

$L$  = Lens Loss (as a ratio) see section 3.3.3

Note: For the cold load thermocouple, equation (a) should be used with data taken in 1979, while equation (b) should be used with data taken in 1980.

## (2) Radiometric Image Data

Data from the first row of the scenes scanned will immediately follow the initial calibration. Each row will normally contain 43 pixels and is always preceded by the ASCII row event marker "ROWXX,NN", where XX denotes the number of the row in BCD (01-99) and NN is the number of pixels in the row also in BCD. Data from each of the eight channels are recorded consecutively with the same channel order as in the calibration block. Table A4 gives the channel order for each pixel. Each 12 bit number represents the output voltage from the radiometer's phase sensitive detector in the range of 0 to 10 volts. Equation 3 in Table 10 will convert these values into brightness temperatures using the calibration data, and Equation 4 will convert them to true scene radiometric temperatures.

The final calibration data will follow the last row of radiometer data and is marked with the ASCII string "CALIB33". Following the last calibration data the remainder of the record will contain zeros with the exception of the last seven bytes which will contain the ASCII string "EOFXXXX" where XXXX is the ASCII frame number.

### d. Tape Compatibility on Other Computers

Data tapes produced by the DCP should be readable by any computer system equipped with an IBM format compatible, nine track, 1600 BPI tape drive. In general a Fortran read statement will be used to transfer data from the tape into the computer's memory. This data will be accessed via an array in Fortran. Each element in the array will generally be a single CDC data word of 60 bits for integer arrays. To unpack the data into 8 bit bytes a combination of Fortran logical operations can be used or some library function may be available. After this it should be a simple procedure to convert ASCII data into code for printing header records and to unpack the binary video and radiometric data based on the format supplied.

Table A4. Radiometer Channel Designations

<u>Channel No.</u>	<u>RF Channel</u>
0	95 GHz, wide band, vertical polarization
1	95 GHz, narrow band, vertical polarization
2	95 GHz, narrow band, horizontal polarization
3	95 GHz, wide band, horizontal polarization
4	Unused
5	Unused
6	Unused
7	220 GHz